Mid-Cretaceous crustal extension recorded in deep-marine half-graben fill, Cedros Island, Mexico

DOUGLAS P. SMITH*
CATHY J. BUSBY } *Department of Geological Sciences, University of California, Santa Barbara, California 92706*

ABSTRACT

Marine, mid-Cretaceous fore-arc strata on Cedros Island (Vargas and Pinos Formations) record the onset of extensional brittle deformation of the upper crust concomitant with initial uplift of blueschist-grade rock from great depth. The pre-extensional Vargas Formation is chiefly fine grained, and it contains facies interpreted as basin-plain, sand-rich–fan, and slope deposits that onlapped a Jurassic unconformity toward the north. The syn-extensional Pinos Formation is coarser grained than is the Vargas and records the initiation and filling of a northeast-southwest–trending, deep-marine, half-graben structure that formed by reactivation of a Jurassic fault zone located along the northern margin of the basin. The axis of the half graben acted as a submarine canyon that funneled gravelly sediment-gravity flows toward the southwest, whereas the shoulder of the half graben was draped by sandy turbidites and mud. A second episode of faulting on a fault parallel to, and synthetic with, the older half-graben fault produced a stress-transfer zone that steepened the intervening block, producing a catastrophic slope failure in the basin.

Several points of evidence suggest that the canyon-bounding fault zone mapped at the northern margin of the basin was syndepositionally active. Basin-floor scarps are indicated by the presence of large, angular blocks derived from the Jurassic strata; these blocks occur within Cretaceous conglomerate and olistostromes, and as clast-supported breccia. Asymmetric basin subsidence is recorded in monotonic lithofacies trends that occur laterally away from the inferred fault zone. These trends include a decrease in average grain size and bed thickness, and an increase in interbedded mudstone and in lateral continuity of individual beds. Abundant slope-failure features, including slide blocks as much as 100 m wide by 40 m thick, also point to frequently recurring intrabasinal seismicity.

The facies distribution and basin structures exposed on Cedros Island are analogous to aspects of the southern Viking Graben and the Ebro turbidite complex. Modern tectonic and physical analogues for the half graben are found at the Kuril margin and in the Aleutian arc, where oblique convergence has produced fault-bounded submarine canyons of the same lateral and vertical scale as inferred for the Cretaceous basin on Cedros Island.

The temporal coincidence between brittle deformation in the upper plate with peak blueschist metamorphism in the lower plate of the convergent margin suggests that initial blueschist uplift began soon after deepest burial.

*Present address: Geology Department, Vanderbilt University, Nashville, Tennessee 37235.

INTRODUCTION

Rocks of western central Baja California (Fig. 1) constitute some of the best exposures of accreted Mesozoic basement, overlap sequence, and high-pressure subduction complex rocks found along the southwestern margin of the Cordillera. On Cedros Island, those three rock types are well exposed in proximity, making possible a study of their genetic relationships (Fig. 1). The mechanisms and rates of blueschist uplift at convergent margins are not well understood. Uplift rates must be high enough to preserve pristine blueschist-mineral assemblages found in some terranes, yet low enough to be driven by assumed rates of underplating. Although most workers agree that blueschists are conveyed upward via underplating and extension of the plate margin (for example, Platt, 1986), uplift rates (which may help to eliminate certain structural uplift models) are not well established.

A tight temporal link between the age of brittle extension in the upper plate and the age of peak blueschist metamorphism in the lower plate, now exposed through structural windows on Cedros Island, strongly suggests a genetic association between the two events. The brittle deformation reported here is consistent with general models proposed for blueschist uplift (for example, Platt, 1986) and supports the geochronologically derived uplift initiation suggested for the Cedros Island blueschist rocks (Baldwin and Harrison, 1989).

Our work shows that mid-Cretaceous strata (Valle Group) on Cedros Island (Fig. 1) record the initiation and filling of an extensional, fault-bounded basin (half graben) that was the locus of rapid, coarse-grained, deep-marine sedimentation from Cenomanian to at least Coniacian time. The half-graben structure was bounded on the north by a southeastward-dipping normal fault, with the greatest accumulation of sediment on the downthrown block, which gently tilted back toward the fault. Extraordinary outcrops on Cedros Island include views of (1) a pre-extensional, sand-rich submarine-fan system; (2) syn-extensional turbidite systems with submarine-canyon, submarine-fan, and slope-apron affinities, deposited within the half-graben structure; (3) footwall rocks of Jurassic age that are recognized as the source of large clasts in the Cretaceous basin fill; and (4) basin-bounding faults of the half graben.

Although this basin subsided in a fore-arc setting, the lithofacies distribution and basin structure are useful as a case study analogous to small, tectonically active, deep-marine basins in rift settings as well. The half-graben fill on Cedros Island might provide an outstanding

Data Repository item 9312 contains additional material related to this article.

Geological Society of America Bulletin, v. 105, p. 547–562, 11 figs., April 1993.

outcrop analogue for models of subsurface facies distributions in the Upper Jurassic Brae Formation of the southern Viking Graben, North Sea (Stow and others, 1982; Harris and Fowler, 1987; Turner and others, 1987). In particular, the exposures on Cedros Island include a small, synthetic, overlapping transfer zone between half-graben–margin splays such as those documented in the graben margin of the East African rift; these features are of interest because they form important hydrocarbon prospects in the North Sea (Morley and others, 1990).

TECTONIC SETTING OF CRETACEOUS STRATA IN WESTERN CENTRAL BAJA CALIFORNIA

Mesozoic rocks of western central Baja California contain a complex but exceptionally complete history of convergent-margin tectonics. An assemblage of Triassic and Jurassic paleo-oceanic terranes, including island-arc, ophiolitic, and blueschist rocks, was accreted to the North American continental margin by late Mesozoic time (Jones and others, 1976; Gastil and others, 1978; Boles and Landis, 1984; Kimbrough, 1985; Moore, 1985; Smith and others, 1991). Subduction jumped outboard of the accreted basement complex, trapping it in the arc-trench gap. The basement diachronously foundered to bathyal marine depths along its length during Early Cretaceous time as it became the floor of an elongate fore-arc basin filled mainly by sediment derived from a continental arc (Fig. 1; Barnes, 1984; Patterson, 1984; Busby-Spera and Boles, 1986). During convergence, subducted oceanic lithosphere reached peak blueschist metamorphism in mid-Cretaceous time and was likely accreted to the base of the upper plate (Sedlock, 1988b; Baldwin and Harrison, 1989, 1992).

The fill and floor of the fore-arc basin are pervasively cut by normal faults likely related to exhumation of blueschist rocks; however, northwest-southeast–trending faults on Cedros Island (see San Agustín [SAF] and Vargas [VF] faults of Fig. 1) are on strike with, and subparallel to, the Tosco-Abreojos fault zone, which formed the North American–Pacific plate boundary from 12 Ma to 5 Ma (Spencer and Normark, 1989). The Vargas and San Agustín faults likely accommodated some right-lateral shear associated with the Neogene plate boundary. Despite the abundance of faults in the Cretaceous section, near coincidence of *in situ* paleomagnetic declinations measured in the northern and southeastern outcrop belts (Fig. 1) precludes the presence of differential tectonic rotations that would adversely affect paleocurrent direction comparisons of the following basin analysis (Smith, 1991).

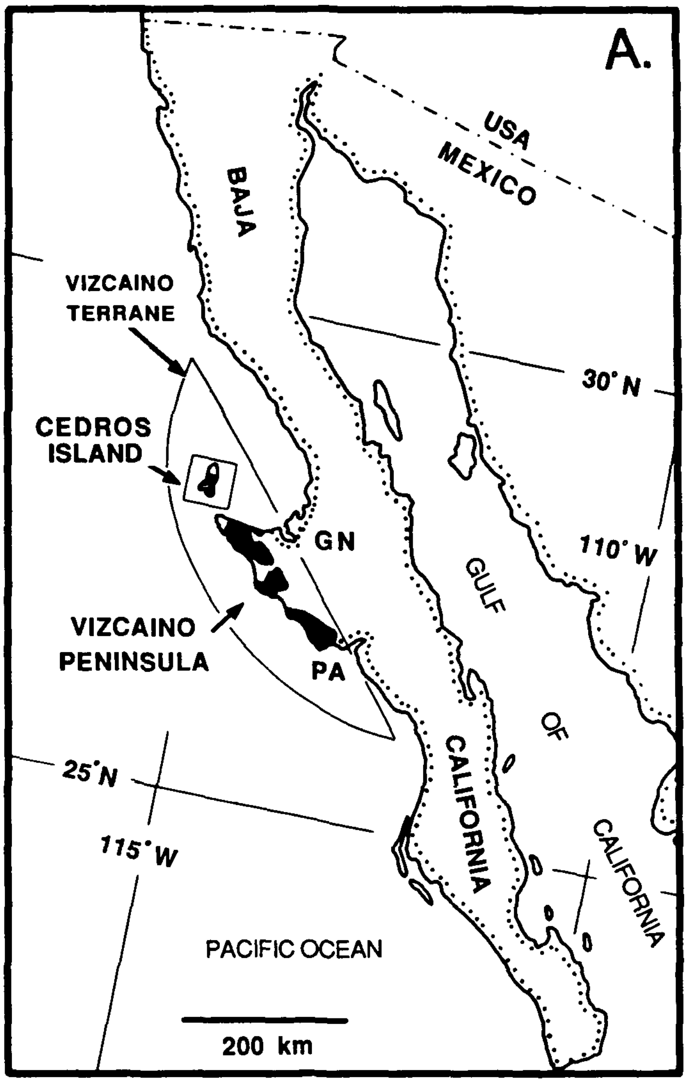

Figure 1. (A) Location of Cedros Island, at the northern end of the Valle Group outcrop belt (black). Mid-Cretaceous continental arc extends from north of the international border southward along the length of the Baja California Peninsula.

LITHOSTRATIGRAPHY

The Valle Group of Cedros Island is divided into the Vargas and Pinos Formations, each comprising several mappable lithologic units (Figs. 2, 3, 4, 5; Smith and others, in press). The Vargas Formation is divided into lower and upper mudstone units that are separated by a sandstone-conglomerate unit (Fig. 2). The Vargas thickens southward from a pinch-out near the mouth of Gran Cañon (Fig. 3) to at least 1,700 m, in about 15 km of lateral distance (Fig. 2). The Vargas Formation progressively lapped northward onto a gently inclined angular unconformity above Jurassic strata from late Albian to early Cenomanian time (Figs. 2, 5). The Pinos Formation includes a broad spectrum of lithofacies that generally are coarser grained than those of the Vargas Formation. The Pinos Formation lies unconformably above Jurassic strata near Arroyo Choyal (Fig. 3), and elsewhere it overlies the Vargas Formation on a diachronous, locally erosive contact that is younger in the south (Figs. 2, 5). The Pinos Formation includes several lithologic units (Fig. 2), but much of the formation remains undivided owing to a poverty of continuously mappable strata. Lateral lithofacies discontinuities arise from faulting and from penecontemporaneous slumping that both removed strata and formed large-scale slump deposits (Fig. 3). The total thickness of the Pinos Formation is unknown, but it likely exceeds 1,500 m.

PALEOBATHYMETRY

The Valle Group on Cedros Island was deposited in outer neritic to bathyal-depth marine waters. Foraminiferal samples from the strata are consistently interpreted as outer neritic to bathyal-depth fauna (Smith and others, in press). Preservation of calcareous species in most samples suggests deposition above the carbonate compensation depth. Shallow-marine mollusks occur as broken and transported

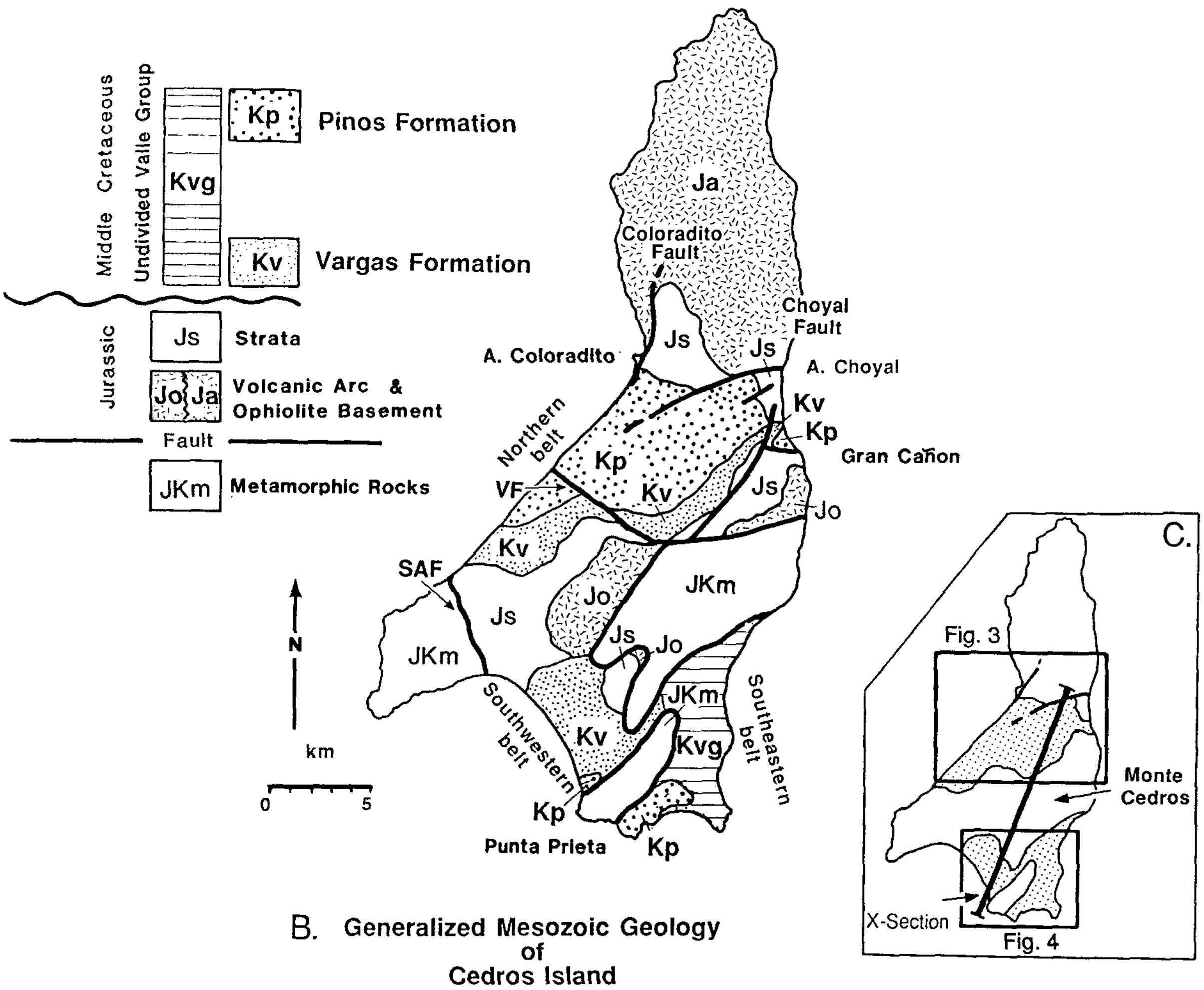

Figure 1. (*Continued*). **(B) Mesozoic units of Cedros Island (modified from Kilmer, 1984). Valle Group strata on Cedros Island are distributed in northern, southwestern, and southeastern outcrop belts. Jurassic strata (Js: volcaniclastics and sedimentary mélange) form the basin floor for the Valle Group. The basement below the Jurassic strata is a Jurassic island-arc complex (Ja) north of the Choyal fault, and a Jurassic ophiolite assemblage (Jo) south of the fault. Jurassic-Cretaceous blueschist-grade metamorphic rocks (JKm) structurally underlie the Jurassic-Cretaceous succession just described. VF and SAF mark the Vargas and San Agustín faults, respectively. (C) Localities of Figures 4 and 5 and approximate trace of projection plane for cross sections (Figs. 2, 6). Outcrop area of Valle Group stippled.**

individuals or within fossiliferous clasts, and so they do not reflect ambient paleobathymetry (examples on loan to Los Angeles County Museum of Natural History). Other biota include ubiquitous woody-plant fragments that occur dispersed in beds and as concentrated layers as much as 10 cm thick. The lack of beds with hummocky cross-stratification or bi-directional cross-laminations, and the abundance of sediment-gravity flows suggest deposition below storm-wave base, seaward of the outer shelf.

SEDIMENTOLOGY

The Vargas and Pinos Formations record a three-phase sedimentologic history beginning in late Albian time, and lasting until at least Coniacian time (Figs. 5, 6). *Phase one* deposits (Fig. 6A) include slope, sand-rich submarine-fan, and basin-plain environments, which represent proximal to distal aspects, distributed north to south, respectively, of one turbidite system (*sensu* Mutti and Normark, 1987). Phase one lasted from late Albian to early Cenomanian time (Fig. 5), but the slope and submarine fan were active only in early Cenomanian time. *Phase two* deposits (Fig. 6B) were deposited on the hanging wall of a half-graben structure bounded on the northwest by penecontemporaneous scarps of the Choyal fault (Figs. 3, 6B). The half-graben floor is divided into axis, proximal-shoulder, and distal-shoulder environments distributed from north to south, away from the Choyal fault (Figs. 5, 6B). The half-graben axis acted as a submarine canyon to direct sediment-gravity flows longitudinally. These environments were active in early Cenomanian time (Fig. 5). *Phase three* deposits (Fig. 6C) include a channel-interchannel system resembling an "inner-fan" submarine-fan environment (*sensu* Mutti and Ricci Lucchi, 1972), and interstratified slope-apron deposits. The slope apron received thick slump deposits shed from an unstable muddy slope. The phase three deposits span early Cenomanian(?) to at least Coniacian

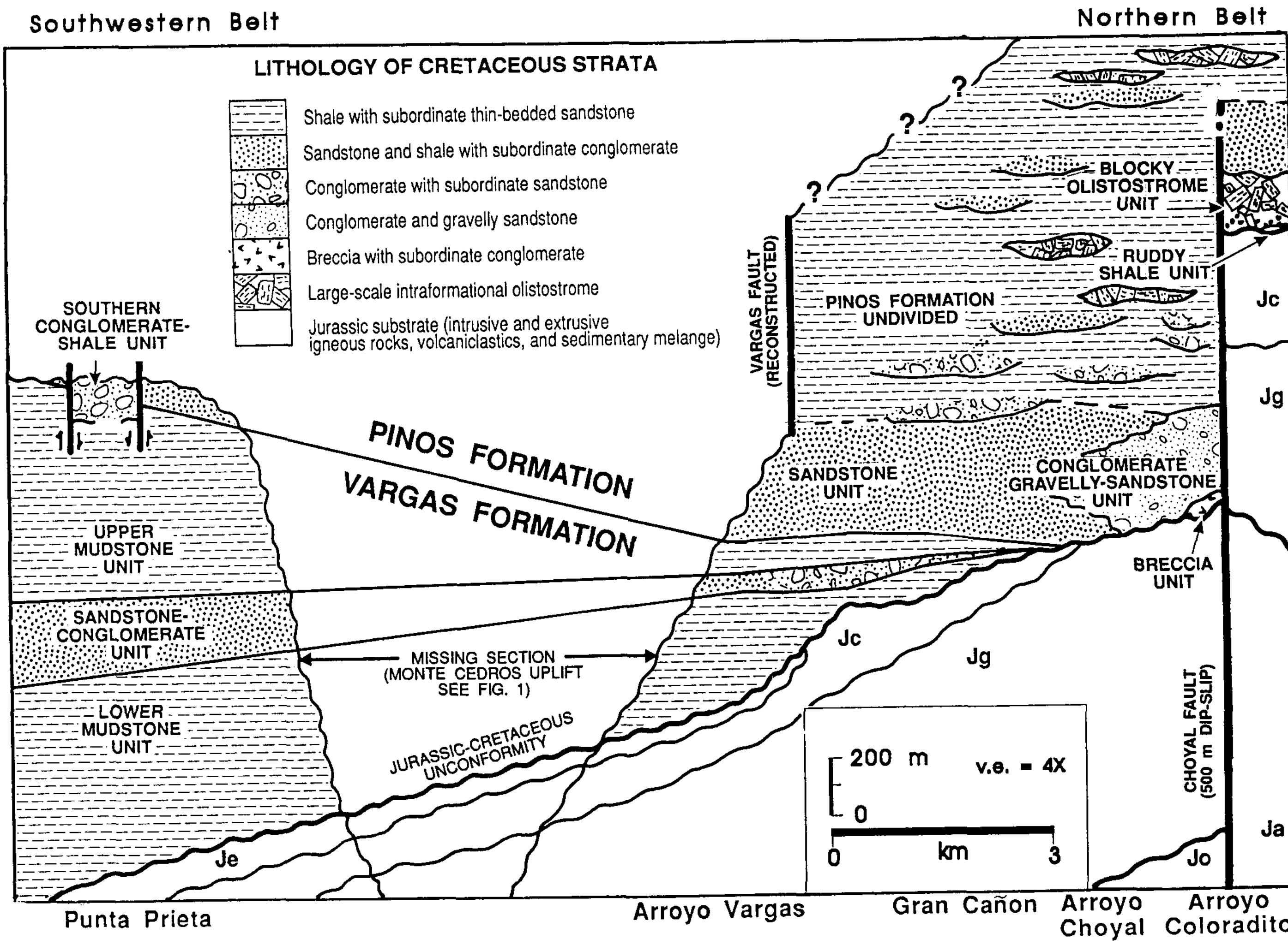

Figure 2. Lithostratigraphy and generalized facies distribution of the Cretaceous Valle Group on Cedros Island (section orientation in Fig. 1C). Top of the sandstone-conglomerate unit of the Vargas Formation is the datum for the cross section. All Cretaceous units shown to the right of the Choyal fault belong to the Pinos Formation, except the ruddy shale unit of the Vargas Formation. Jurassic basement units are as in Figure 1. Jurassic strata are divided into the following: Jg: volcaniclastic strata of the Gran Cañon Formation (Kilmer, 1984; Kimbrough, 1984; Busby-Spera, 1988); Jc: sedimentary mélange of the Coloradito Formation (Boles and Landis; 1984; Kilmer, 1984); Je: marine volcanogenic conglomerate of the Eugenia Formation (Kilmer, 1984; Boles and Landis, 1984).

time, and they include evidence for activity on a second syndepositionally active fault (Coloradito fault; Figs. 3, 6C).[1]

Phase One: Basin-Plain, Slope, and Sand-Rich Fan (Late Albian to Early Cenomanian)

Phase one deposits include the lower mudstone, sandstone-conglomerate units, and the lowest 100 to 150 m of the upper mudstone unit of the Vargas Formation (Fig. 2). The lower mudstone unit records the onset of Valle Group deposition on Cedros Island in a basin-plain environment. The overlying sandstone-conglomerate unit and lowest 100 to 150 m of the upper mudstone unit (Fig. 2) grade from slope deposits in the north to sand-rich submarine fan and superposed basin-plain environment, respectively, in the south (Figs. 5, 6A).

Basin-Plain Deposits. The lower mudstone unit records deposition in a sand-impoverished basin-plain environment that lapped northward onto a gently southward-inclined unconformity (Fig. 2) between late Albian and early Cenomanian time (Figs. 5, 6A). The lower mudstone unit is chiefly parallel-laminated siltstone-mudstone couplets, with the siltstone laminations commonly rippled or bearing small-scale cross-laminations (facies 5a, 6a, 6b; Table 1). Thin-bedded, fine-grained, graded sandstone beds are rare. The beds and laminations are laterally continuous beyond the limits of most unfaulted sections of outcrop (>100 m). These facies record deposition by dilute turbidity currents and hemipelagic sedimentation (Pickering and others, 1986).

[1]GSA Data Repository item 9312 (Tables 1, 2, and 3, containing detailed sedimentological facies descriptions) is available on request from Documents Secretary, GSA, P.O. Box 9140, Boulder, CO 80301.

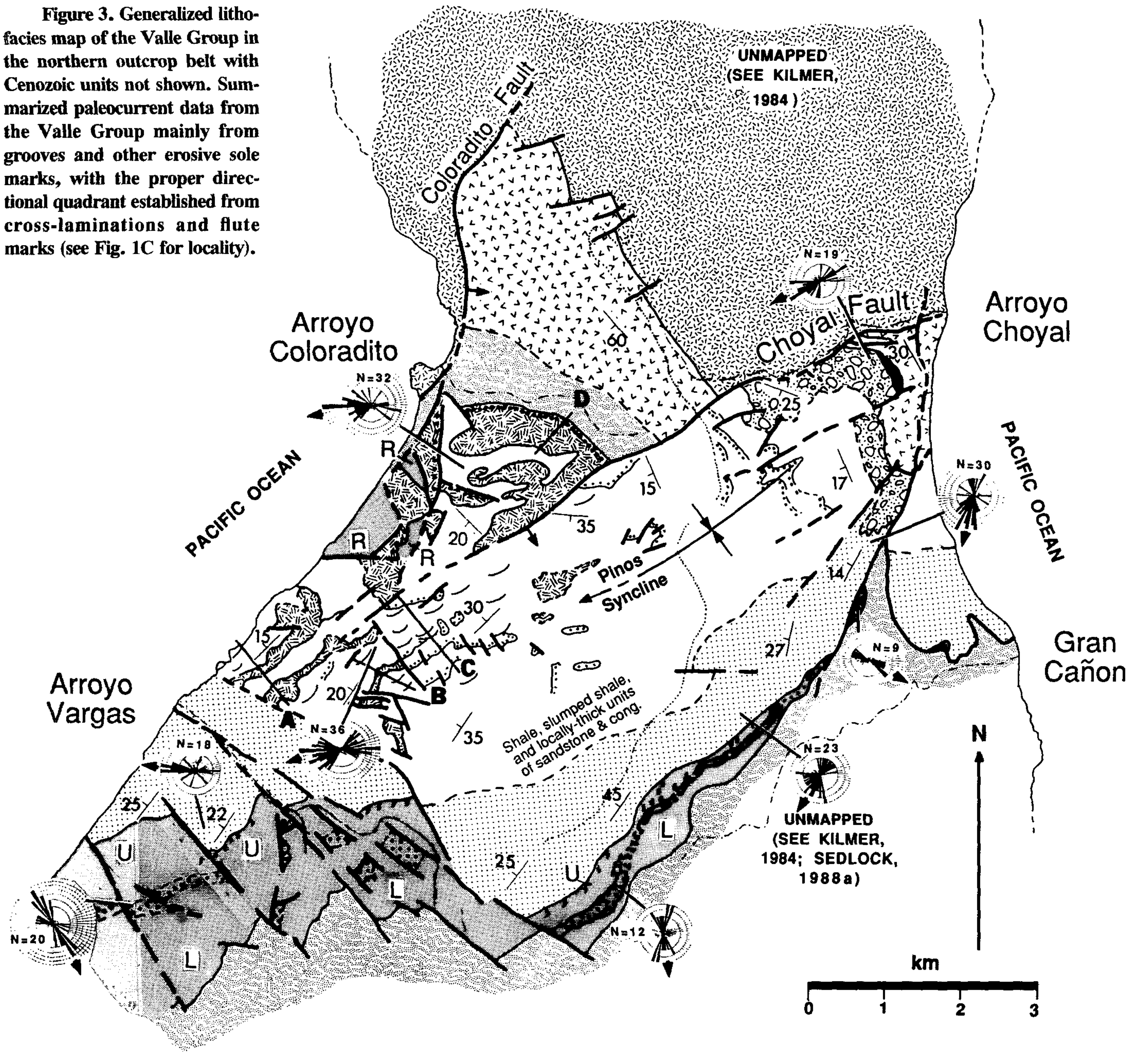

Figure 3. Generalized lithofacies map of the Valle Group in the northern outcrop belt with Cenozoic units not shown. Summarized paleocurrent data from the Valle Group mainly from grooves and other erosive sole marks, with the proper directional quadrant established from cross-laminations and flute marks (see Fig. 1C for locality).

Weak bottom currents commonly reworked the sediment into small-scale ripples. The paucity of both soft-sediment deformation and coarse-grained sediment-gravity flows in this unit suggests a sand-starved, basin-plain environment (Mutti and Ricci Lucchi, 1972).

Slope Deposits. In the northern part of the basin, the sandstone-conglomerate unit and upper mudstone unit were deposited in a slope environment (Figs. 5, 6A). The sandstone-conglomerate unit in this area comprises stacked conglomerate beds that fill steep-sided channels. The channels typically cut down into a 2- to 20-m-thick, upward-thickening sequence of sandstone beds and are filled with a variety of conglomerate facies (facies 2a, 2b, 2c, 2d; Table 3), slump deposits (facies 1d; Table 2), and pebbly mudstone. Channel fills are commonly capped by a 1- to 3-m-thick, upward-thinning sequence of sandstone beds. These channels are discontinuous, with the intervening deposits rich in contorted mudstone and pebbly-mudstone (facies 1d and 1e; Table 2). The upper mudstone unit consists of parallel-laminated mudstone and thinly interbedded sandstone (facies 6b and 5a; Table 1) that locally are slumped (facies 1c, 1d, and 1e; Table 2). In some parts of the upper mudstone unit, the mudstone and sandstone beds pinch out against small channels or scours that reach several meters in width and 1 to 2 m in depth.

The sandstone-conglomerate unit in the northern part of the basin lies stratigraphically above basin-plain deposits (lower mudstone unit) and below slope deposits (upper mudstone unit); it records the filling of steep-sided channels in a slope environment. A system of coeval channels were cut into sand lobes that prograded into this part of the

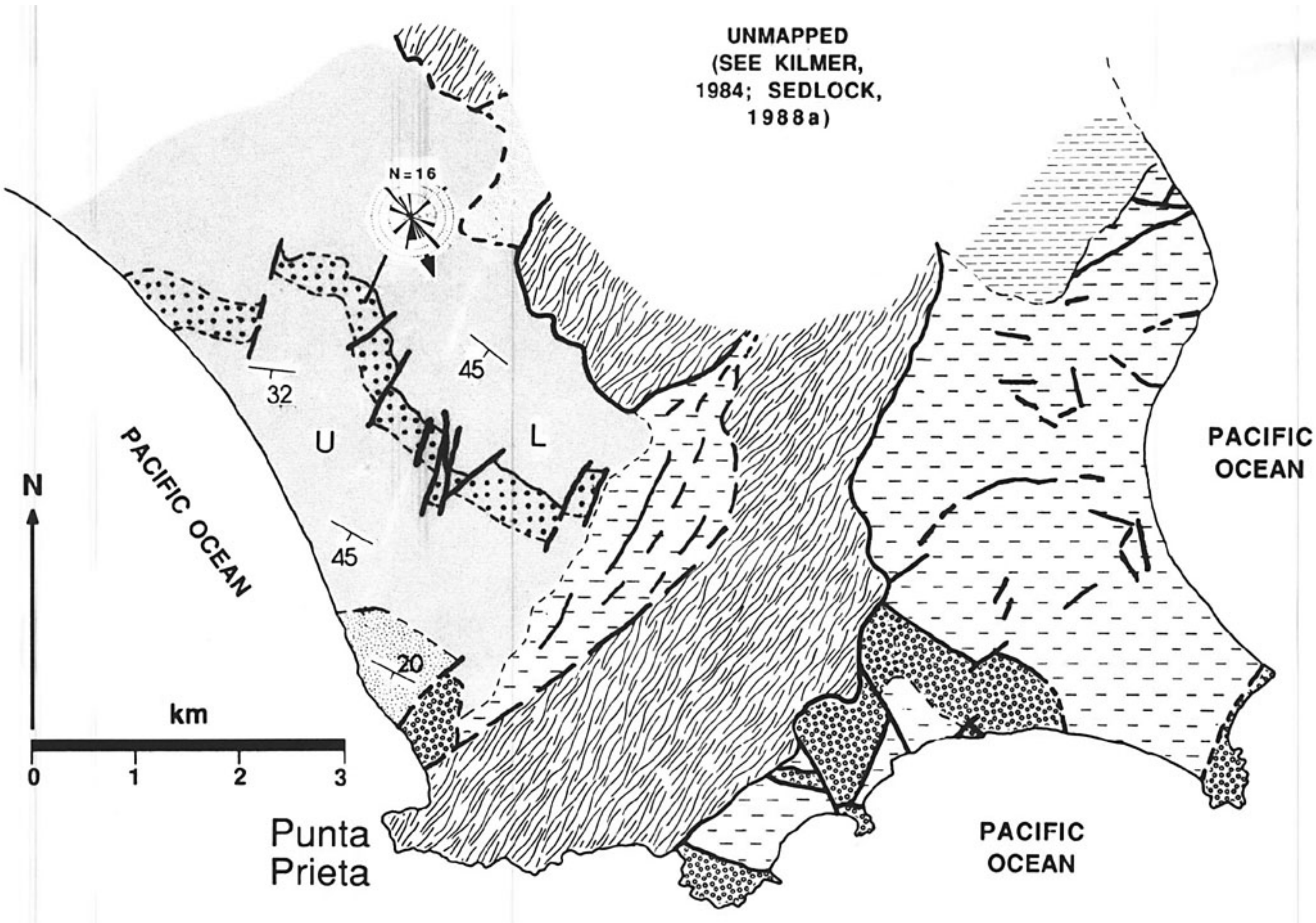

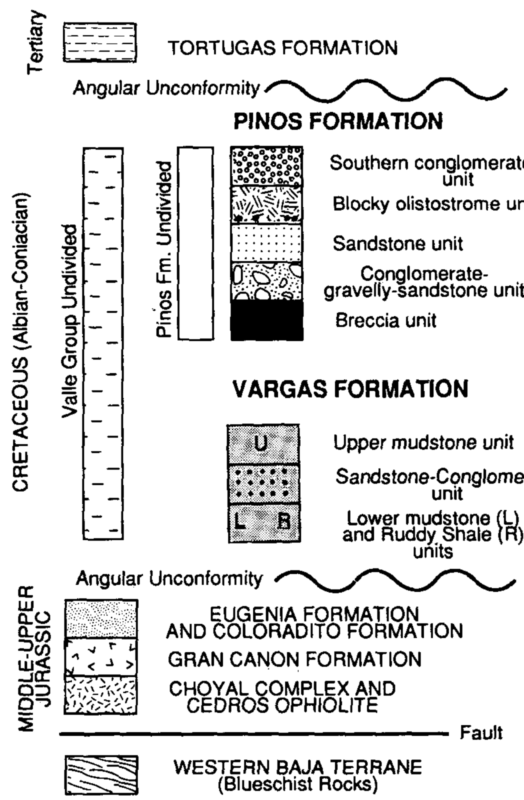

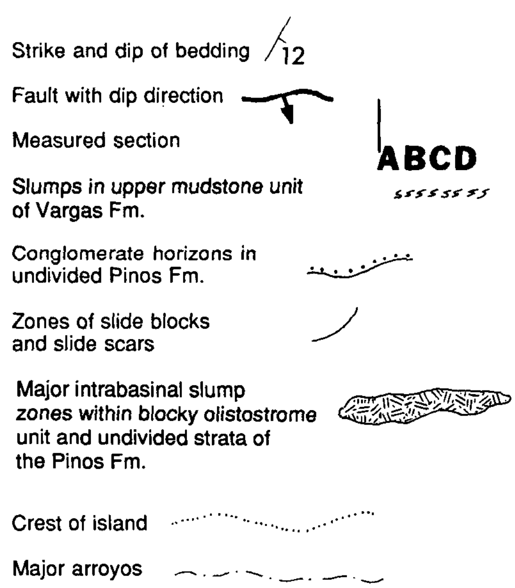

Figure 4. Generalized lithofacies map of the Valle Group in the southwestern and southeastern outcrop belts with Quaternary deposits not shown (see Fig. 1C for locality).

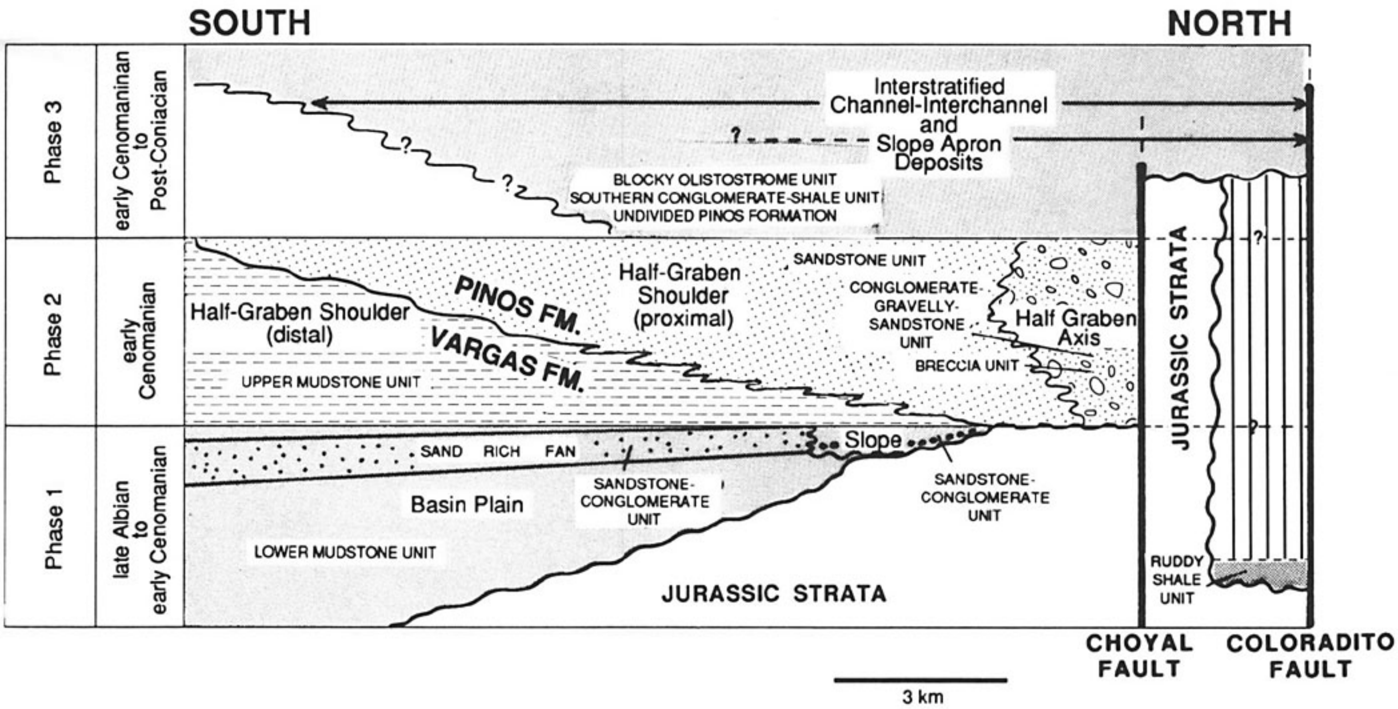

Figure 5. Late Albian to Coniacian lithostratigraphic units of the Valle Group on Cedros Island (Figs. 2, 3, 4) record a three-phase basin evolution (see Fig. 1C for profile orientation; no vertical scale implied; see Fig. 2 for thicknesses of units). Paleocurrents for phase one deposits are out of the page to the left, whereas they are into the page and to the left for phase two and phase three deposits (Figs. 3, 4).

basin (Fig. 6A). The upper mudstone unit contains scoured hollows that are draped by thin turbidites and mudstone, indicating that the flows producing the scours did not fill them, but continued farther downslope. Such sediment bypass should be typical of slope environments. The interstratified slumped mudstone and steep-sided channels are typically ascribed to a slope environment as well (Mutti and Ricci-Lucchi, 1972). Upward-thickening bedding sequences like those beneath the channels are not commonly ascribed to a slope environment, but are generally interpreted as sand lobes in turbidite systems of the rise (Mutti and Ricci Lucchi, 1972), and so they may represent the rise component of a local plain-rise-slope progradational sequence.

Sand-Rich Submarine-Fan Deposits. In the southernmost part of the northern outcrop belt and in the southwestern outcrop belt (Figs. 3, 4), the sandstone-conglomerate unit is a sand-rich submarine fan interstratified between basin-plain mudstone of the lower and upper mudstone units (Figs. 5, 6A). The sandstone-conglomerate unit in these areas is a mudstone-poor wedge of bedded sandstone that grows in thickness from about 40 m in the north to more than 200 m thick in the south (Fig. 2). In the south, it forms long topographic ridges containing laterally continuous, fine- to coarse-grained, graded and nongraded, thin- to thick-bedded sandstone (facies 3 and 7; Table 1). The sandstone beds have scoured, flat bases; range in thickness from a few centimeters to 6-m-thick amalgamated beds, with most less than 1 m; and range from being massive to having full Bouma sequences, with the former more common. Both upward-thinning and upward-thickening bedding sequences 2 m to 4 m in thickness are present, and the whole unit fines and thins upward, concomitant with an increase in the proportion of mudstone interbeds. The sandstone unit abruptly overlies the lower mudstone unit, but its top is gradational into the upper mudstone unit for more than 2 m to several tens of meters. Sandstone beds of the sand-rich submarine fan were deposited from both high- and low-density turbidity currents. The largest rip-up clasts (up to 1.5 m long), which are locally present at the base of the unit, record the erosion of the muddy substrate by the first turbidity currents cascading into the basin. There is weak evidence of turbidite aggradation by both lobe-building (upward-thickening bedding sequences) and channel-filling (upward-thinning sequences, minor 1- to 2-m-thick slump horizons, and mudstone rip-up clasts) processes, working in the basin at different times.

The short-lived sand-rich submarine fan described here differs from the family of submarine-fan models that evolved from the seminal work of Mutti and Ricci Lucchi (1972) in that it shows no evidence for initial gradual progradation across the basin plain. Another aspect that differs from those models is that there is no channel-levee complex intervening between the fan deposits and coeval slope channels to the north that likely sourced the fan (Fig. 6A). These two aspects make the fan akin to "poorly efficient," sand-rich turbidite systems (Mutti, 1979), typically described from small, tectonically active basins in both ancient and modern examples (Normark and others, 1979; Graham and Bachman, 1983; Link and Nilsen, 1980; Busby-Spera, 1985; McClean and Howell, 1985).

Phase Two: Axis and Shoulder Deposits of a Half-Graben Fill (Early Cenomanian)

Phase two deposits include the breccia unit, conglomerate–gravelly sandstone unit, and sandstone unit of the Pinos Formation, and the upper part of the upper mudstone unit of the Vargas Formation (Figs. 2 and 5). The breccia unit and conglomerate–gravelly sandstone

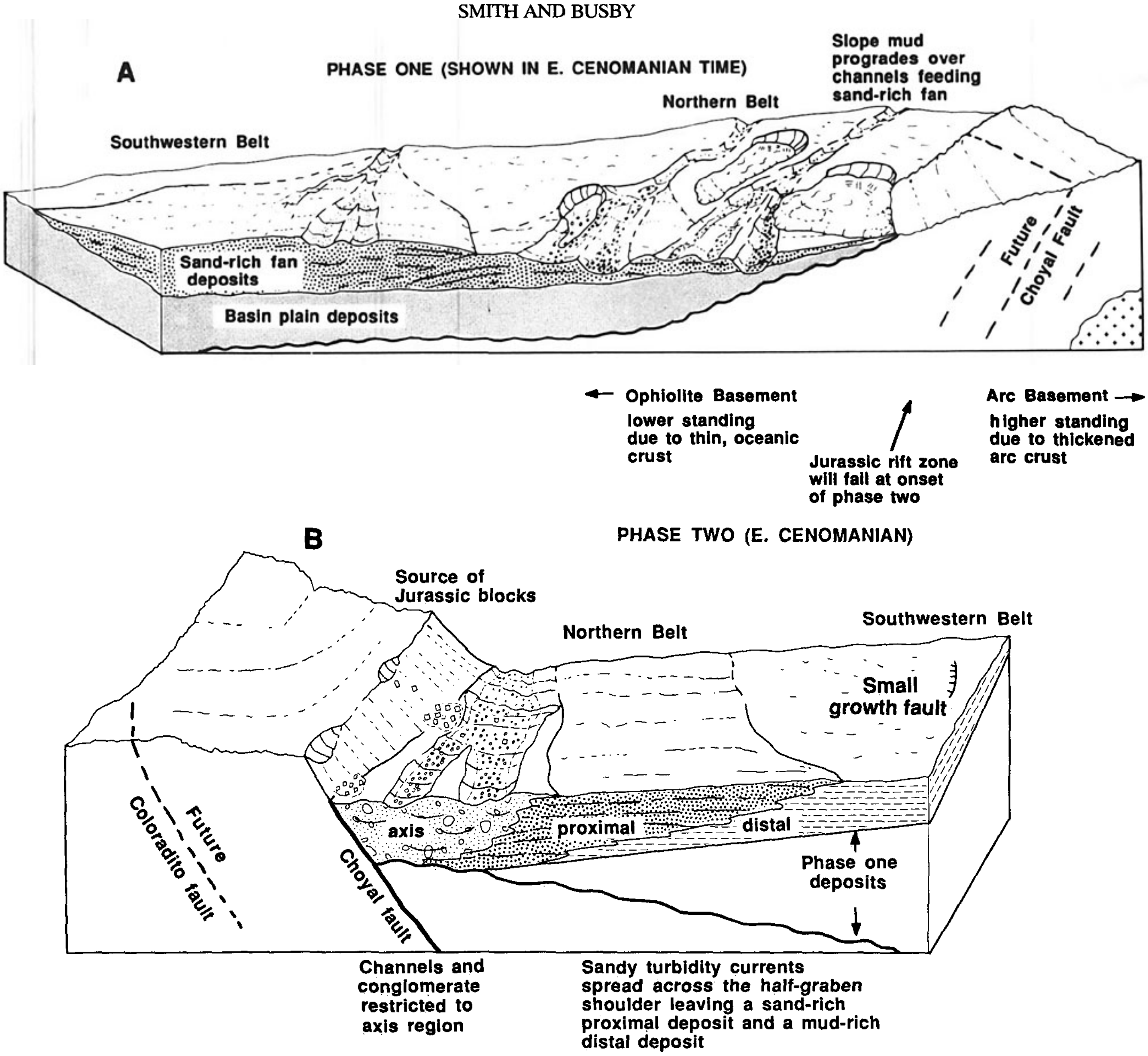

Figure 6. Paleogeographic reconstructions of the three phases of basin evolution. (A) Phase one depositional environments with view approximately toward the west. (B) Phase two depositional environments with view approximately toward the northeast.

units filled the axis of a longitudinally drained half graben, bounded on the northwest by the Choyal fault, whereas deposits of the sandstone unit and upper mudstone unit draped proximal and distal parts, respectively, of the down-dropped half-graben floor (Fig. 6C). The shoulder deposits extend from about 3 km south of the Choyal fault to the southwestern outcrop belt, a distance of about 15 km (Fig. 5). In descriptions of phase two deposits, the terms "proximal" and "distal" are used with respect to the Choyal fault, along a north-south traverse, obliquely down paleocurrent (Figs. 1C, 5).

Half-Graben Axis Deposits (Axial Submarine Canyon). The breccia unit of the Pinos Formation (Fig. 2) was deposited as a talus cone. The breccia forms a 75-m-thick by 500-m-wide deposit extending southward from about 150 m south of the Choyal fault (Figs. 2, 3). The unit is a clast-supported deposit of large (up to 13 m long), angular blocks, sourced from the underlying Middle Jurassic units (facies 1a; Table 2). The breccia rests atop a steep-sided scour in the Jurassic strata, and it interfingers with the conglomerate–gravelly sandstone unit. The breccia deposit is matrix-poor, making *en masse* transport by debris-flow processes unlikely; an origin as a talus pile resulting from noncohesive landslide or rockfall is more probable (compare with facies F1.1 of Pickering and others, 1986). The compositions of blocks in the deposit, which match Jurassic strata in the footwall of the Choyal fault, and the proximity of the deposit to the Choyal fault trace (Fig. 3) suggest that the blocks were shed onto the down-dropped fault block from a footwall scarp of the Choyal fault.

The conglomerate–gravelly sandstone unit of the Pinos Formation is a nearly mud-free unit consisting of conglomerate and gravelly sandstone beds with scoured bases and tops. The conglomerate-sandstone unit forms a 200- to 300-m-thick section above the breccia unit, next to the Choyal fault (Figs. 2, 4, 5). The gravel fraction in the unit

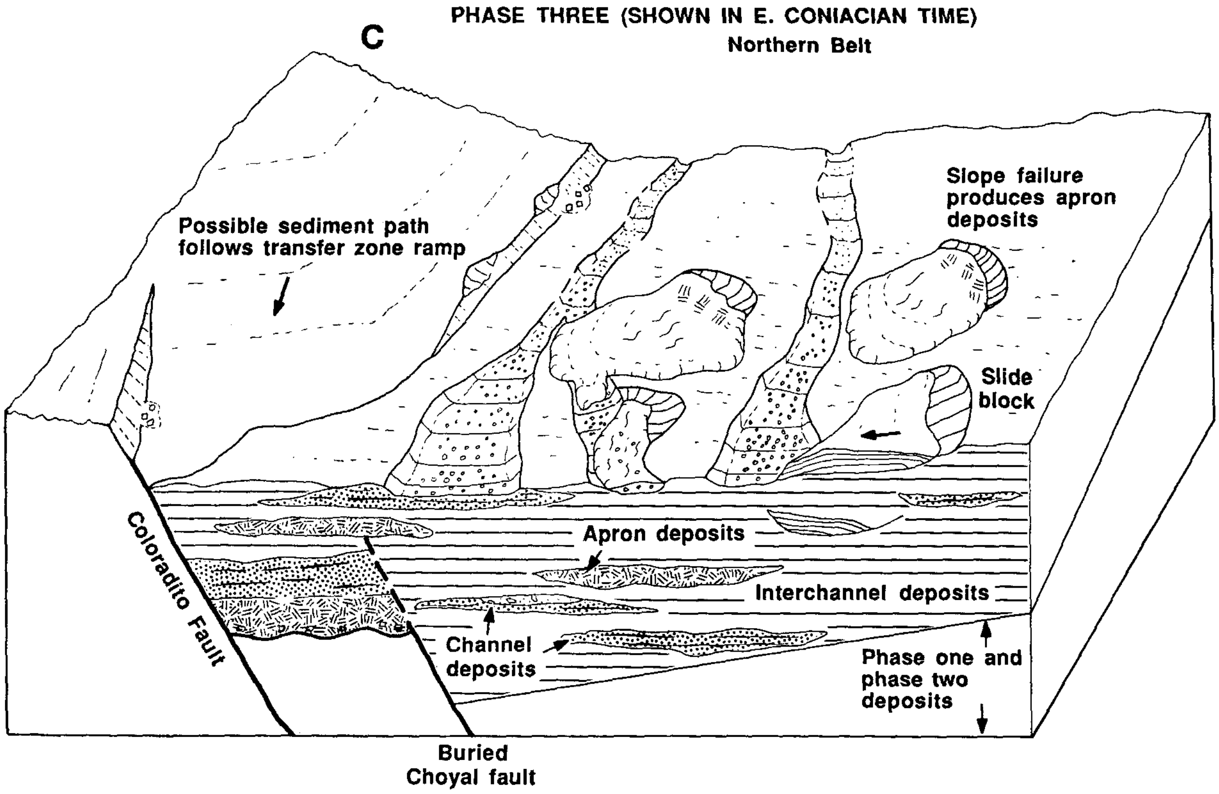

Figure 6. (*Continued*). (C) Phase three depositional environments with view approximately toward the northeast.

consists of rounded, medium-sized pebbles of continental-arc affinity, and angular blocks (as much as 3 m in size) derived from the local Jurassic substrate are present in minor amounts. The conglomerate–gravelly sandstone unit consists of two to three, vertically stacked, laterally discontinuous, 100-m-thick megacycles, each with a 50-m-thick, conglomerate basal interval and a 50-m-thick, gravelly sandstone upper interval. At the southern (distal) margin of the conglomerate–gravelly sandstone unit, about 2 km south of the Choyal fault (Fig. 2), some of the conglomerate beds pinch out, leaving a much increased proportion of gravelly sandstone and sandstone (see "axis" to "proximal" transition in Fig. 6B). Here, many of the sandstone beds are capped by mud-draped scours and are chiefly massive or planar-laminated, with medium- to large-scale cross-laminations also locally abundant.

The conglomerate intervals were deposited by numerous high-density, gravelly sediment-gravity flows (Lowe, 1982). The scoured tops of nearly all beds and lack of significant interbedded sandstone or mudstone indicate that the environment was chiefly a locus of sediment bypass rather than aggradation, except for the coarsest gravel fraction of successive sediment-gravity flows. The gravelly sandstone intervals record periods when either the relative abundance of gravel to sand entering the basin was reduced, or the energy of individual flows was diminished, so that the gravel fraction settled farther upslope.

The half-graben axis deposits record the gradual filling of an axially steep, erosively based, areally restricted, relatively long-lived sediment conduit that we interpret as a structurally controlled submarine canyon (Fig. 6B). These deposits, the most gravel-rich deposits in the basin, are restricted to a 2- to 3-km-wide zone abutting the Choyal fault (Figs. 5, 6B), indicating that the canyon axis was not free to migrate away from scarps of the syndepositionally active Choyal fault zone. Paleocurrents are toward the southwest adjacent to the Choyal fault, parallel to the trend of the Choyal fault (Fig. 3), supporting the idea that flows were directed longitudinally along the axis of the half graben. The presence of large blocks of Jurassic strata throughout the thickness of the axis deposits is evidence that the footwall of the Choyal fault was continually renewed, rather than buried.

The strata at the southern margin of the axial deposits mark the transition from confined flows of the canyon axis to unconfined sheet flows of the half-graben floor. These deposits are located obliquely down paleocurrent from the deposits described adjacent to the Choyal fault (Fig.3). The presence of mud-draped scours near the margin of the axis records sediment bypass, which is a key feature of the "channel-lobe-transition" deposits of Mutti and Normark (1987), whereas the cross-bedding is a feature of the channel-mouth bars of Shanmugam and Moiola (1988). Both the "channel-lobe-transition" and channel-mouth bars are likely to form where turbidity currents leave a relatively high gradient channel, spreading out onto a relatively flatter part of the basin. Although these deposits on Cedros Island do not lead into well-expressed lobe deposits, they do mark the transition from scoured, conglomeratic deposits of the half-graben axis to better-stratified, gravel-poor, sandy turbidites, deposited on the flat floor of the half-graben shoulder described next.

Half-Graben Shoulder Deposits (Proximal). The sandstone unit of the Pinos Formation (Fig. 2) was deposited by sandy turbidity currents that spread laterally across the half-graben floor, away from the axis of the half graben. The unit crops out along most of the northern outcrop belt, and in a small exposure near Punta Prieta (Figs. 3, 4). The sandstone unit is more than 500 m thick, and it includes a wide variety of sediment-gravity-flow deposits. The type section (Smith and others, in press) is mainly medium- to thick-bedded, fine- to medium-grained, planar-laminated, graded and nongraded sandstone beds (facies 3 and 4; Table 1) separated by mudstone laminae or thin beds of ripple-laminated siltstone (facies 6a; Table 1). The sandstone-to-shale ratio is commonly very high (20:1 to 30:1), and some sections are nearly devoid of mudstone. Sandstone-bed geometry ranges from planar with good lateral continuity (>100 m) to lenticular over several meters. Although vertical trends in bedding thickness are not common in the unit, upward-thinning sequences outnumber upward-thickening sequences. Sedimentologic trends occurring with distance away from the Choyal fault include a change from nongraded, medium- to thick-bedded sandstone with poor lateral bed-continuity and a paucity of interbedded mudstone to laterally continuous, graded, thin- to medium-bedded sandstone with a greater proportion of interbedded mudstone. These changes occur rapidly along the 5-km length of Gran Cañon and continue south of Arroyo Vargas (Fig. 3).

There is great sedimentologic diversity in the sandstone unit, and we offer only a generalized view of its formation. Monotonously stacked, graded sandstone beds, which form the vast majority of the association, were deposited by high-density and low-density turbidity currents (Pickering and others, 1986). The paucity of both deep scours and well-developed vertical trends in bed thickness suggests that neither channel-filling nor lobe-progradation processes were important in this part of the basin. The southern edge of this environment gradually migrated southward, as represented by the southward-younging contact between the Pinos and Vargas Formations (Fig. 5).

The position of the sandstone unit, laterally adjacent to the coarser-grained half-graben axis deposits (Fig. 5) suggests that it records the deposits of turbidity currents that lost energy as they spread laterally, away from the axis, ascending the basin floor, which likely had a component of tilt toward the Choyal fault (Fig. 6B). Paleocurrent averages, plotted for three regions in the unit (Fig. 3), tend to wrap from south to southwest to west with distance away from the Choyal fault. This may result from sediment-gravity flows "banking off" (oblique reflection) a basin floor tilted gently to the northwest, toward the Choyal fault.

Half-Graben Shoulder Deposits (Distal). Much of the upper mudstone unit of the Vargas Formation (Figs. 2, 5) was deposited high on the distal part of the half-graben shoulder (Figs. 5, 6B), beyond the reach of most turbidity currents. The upper mudstone unit is chiefly parallel-laminated mudstone that is locally rippled (facies 5a, 6a, 6b; Table 1). In outcrop, the upper mudstone unit is virtually indistinguishable from basin-plain deposits of the lower mudstone unit of the Vargas Formation (see "Phase one" above). The "distal graben shoulder" interpretation stems mainly from their temporal association with faulting along the Choyal fault, and distance from the coarse-grained, axial deposits. The only aspect distinguishing the upper mudstone unit from the lower mudstone unit in these distal deposits is a minor amount of soft-sediment deformation in the upper mudstone unit. Small-scale slump folds, minor load structures, and a small growth fault suggest recurring syndepositional seismicity.

Phase Three: Interstratified Slope-Apron and Channel-Interchannel Deposits (Early Cenomanian? to Post-Coniacian)

Phase three deposits (Fig. 6C) comprise several lithologic units in the Pinos Formation (Fig. 5). These deposits overlie the phase two half-graben deposits, bury the trace of the Choyal fault, and record activity on a second fault, the Coloradito fault (Fig. 3). Phase three deposits are sedimentologically and structurally complex but are characterized as stacked channel-interchannel deposits that are interstratified with thick intrabasinal slump deposits of a slope apron (Figs. 6C, 7).

Channel-Interchannel Deposits. The channel-interchannel deposits are largely thinly interbedded, rippled sandstone and rippled mudstone (facies 5a, 5b, and 6a; Table 1) with interstratified conglomerate (facies 2f, 2b, and 2g; Table 3) or thick-bedded sandstone (facies 3 and 4; Table 3 and Fig. 7).

Interchannel Deposits. The interchannel deposits are much more abundant than the channel deposits. The interchannel deposits (facies 5a, 5b, and 6a; Table 1) occur in units ranging from 20 m to about 100 m in thickness (Fig. 7). They bear both laterally continuous and laterally discontinuous, thin sandstone beds that are commonly erosively based and pervasively ripple laminated. Although the beds are generally thin, they range in grain size from silty, fine-grained sandstone to coarse-grained sandstone, and they commonly contain load casts and flames. These deposits resulted from repeated incursions of dilute, thin, sandy turbidity currents across an environment that was normally receiving hemipelagic clay and silt. Both the sandstone beds and siltstone beds show evidence of fairly continuous, dilute, unidirectional currents. Some of the thin sandstone beds are composed of medium to coarse sand, like "facies E" deposits of Mutti and Ricci Lucchi (1972). The presence of this facies thickly interstratified with coarse-grained (channel) deposits, and the evidence for episodic current reworking, suggest that they are interchannel deposits (Mutti and Ricci Lucchi, 1972) that received thin sediment-gravity flows when confined turbidity currents overtopped the channel bank.

The interchannel deposits bear sediment-failure features at many different scales that may record basin tilting, rather than levee building. The sediment-failure deposits include large (as much as 40 m thick by 100 m wide) slide blocks (facies 1b; Table 2), small-scale slumped layers (facies 1d; Table 2), as well as load structures and flames. In some localities, glide blocks truncate the conglomerate layers (for example, column C of Fig. 7). Slump scars also occur at sporadic intervals in the section (Figs. 7, 3), with some laterally exposed for at least 100 m. Two well-exposed examples of scars are oriented northeast-southwest, arcuate in plan form (concave to the northwest), and dip northwest (toward the fault-bounded basin margin). The scars are filled with pebbly mudstone (facies 1e; Table 2), slumped mudstone (facies 1d; Table 2), and thin- to thick-bedded, graded sandstone (facies 4; Table 1) that lap against the steep scar surface. Although the interchannel deposits include many scales of sediment failure, this does not necessarily demonstrate the presence of levees (*sensu* Mutti and Normark, 1987). This condition could result from at least three causes: (1) the interchannel deposits formed 40-m-tall (minimum height based on thickness of individual slide blocks) levees that episodically failed; (2) the deposits were exposed in 40-m-deep channel banks, undercut to the point of failure by erosive channelized flows; or (3) the interchannel deposits were deposited on a sloping basin floor (half graben), and failed from intrabasinal seismicity or simple oversteepening. It is not easy to distinguish among these possibilities. The presence of slide blocks that pinch out conglomerate beds (column C of Fig. 7) indicates that some of the blocks slid into and likely cut off channel thalwegs from further activity. We cannot demonstrate that slide blocks were also directed away from the channels, which would substantiate the presence of levees (Morris and Busby-Spera, 1990). A tilted half-graben floor (and associated seismicity) would explain the

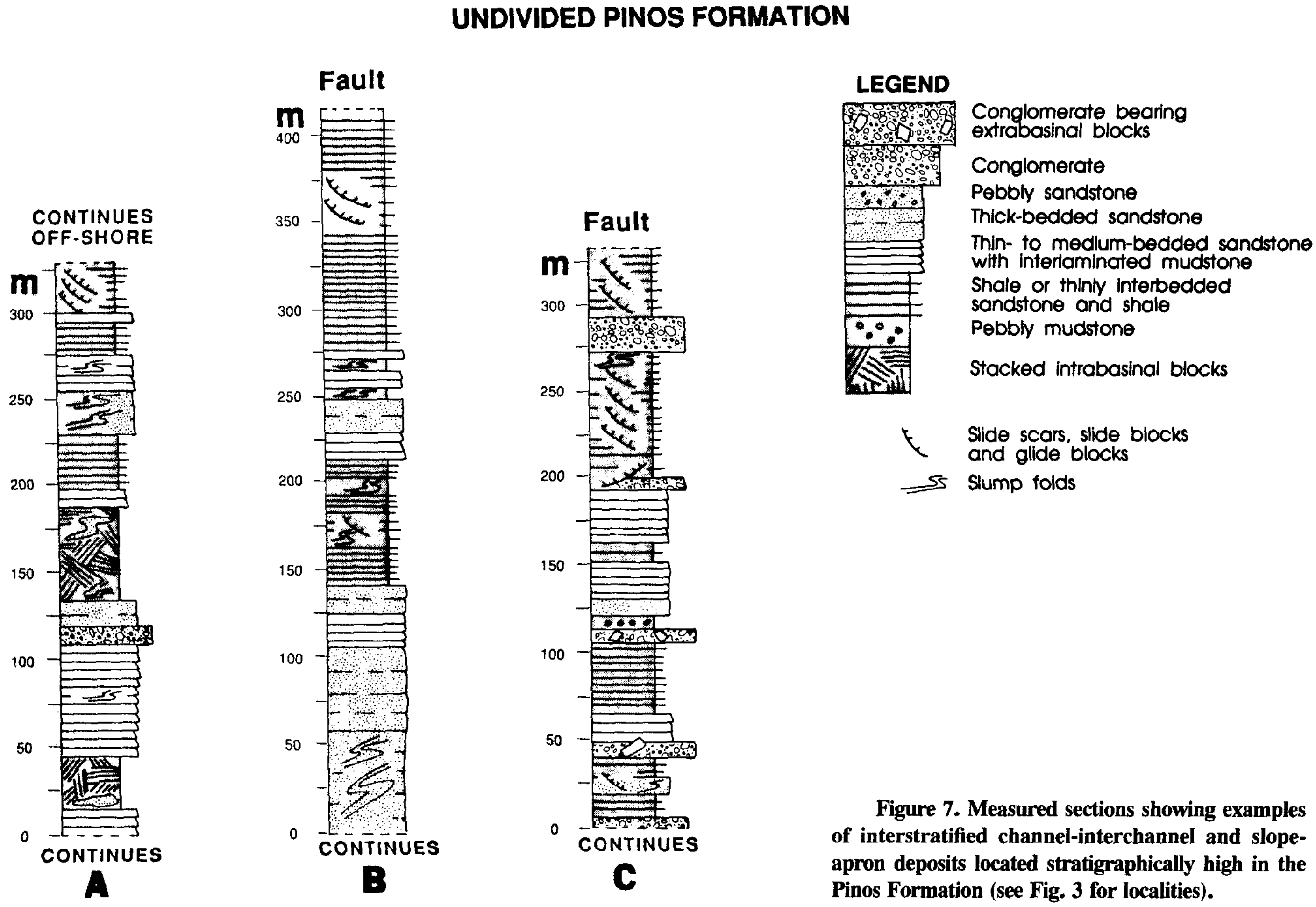

Figure 7. Measured sections showing examples of interstratified channel-interchannel and slope-apron deposits located stratigraphically high in the Pinos Formation (see Fig. 3 for localities).

abundance of sediment-failure features and prevalence of west-north-west–directed slide scars throughout the section (schematically shown in Fig. 3).

Channel Deposits. Conglomerate and thick-bedded sandstone interstratified with the interchannel deposits include both channelized units and more laterally continuous, perhaps nonchannelized deposits. Channel deposits consist of 2- to 20-m-thick units comprising stacked beds of horizontally or cross-stratified conglomerate and pebbly sandstone (facies 2f; Table 3), sandstone-matrix conglomerate with various kinds of grading (facies 2d; Table 3), and mud-matrix conglomerate or slumped mudstone (facies 1d and 2c; Tables 2 and 3). Channel deposits commonly overlie a several-meter-thick, upward-thickening sequence of graded sandstone beds, and are rarely capped by an upward-thinning sequence of beds. Other coarse-grained units, which may or may not be related to channel processes include (1) single- or multiple-event, basement-block–bearing, matrix-rich, disorganized conglomerate units (usually facies 2c or 2a) as much as 20 m thick, but commonly about 2 m to 4 m thick that may or may not fill a basal scour; and (2) sections as much as 100 m thick comprising thick-bedded, massive sandstone (facies 3; Table 1) or thickly interstratified massive sandstone and various slump deposits (facies 1d; Table 2). Both the channel-deposits and other coarse-grained deposits contain abundant Jurassic blocks derived from the basin floor. The Jurassic blocks decrease in size and abundance away from the Choyal and Coloradito faults (Figs. 3, 5), and are absent in coeval deposits far from the faults (southern conglomerate-shale unit, Figs. 2, 4). In all of these coarse-grained deposits, the mud-matrix conglomerate was transported as cohesive debris flows, whereas sand-matrix conglomerate was deposited from high-density turbidity currents (Lowe, 1982; Pickering and others, 1986). The sedimentological origin of the thick, massive sandstone beds is enigmatic, but they may have been deposited from high-density turbidity currents or fluidized flows (Pickering and others, 1986).

Slope-Apron Deposits. Slope-apron deposits include the blocky olistostrome unit of the Pinos Formation, and several large-scale chaotic mudstone deposits within the undivided part of the Pinos Formation (Figs. 2, 3, 5, 6C). The blocky olistostrome unit (Fig. 8) forms a broad (2 to 3 km minimum), 180-m-thick deposit above the Jurassic unconformity between the Choyal and Coloradito faults (Figs. 3, 5). The blocky olistostrome unit grades upward from a basal section of blocky conglomerate (facies 2a; Table 3) to block-bearing, pebbly-mudstone (facies 1e; Table 2), and finally to a section of stacked, intrabasinal slump blocks (Fig. 8; facies 1c and 1d; Table 2). These blocks range in age from early or middle Albian to middle Cenomanian (Smith and others, in press). The younger slope-apron deposits, within the undivided Pinos Formation ("intrabasinal slump" deposits of Fig. 3; Fig. 7) are units of stacked, internally coherent intrabasinal slump blocks (facies 1c; Table 2). The units range in thickness from

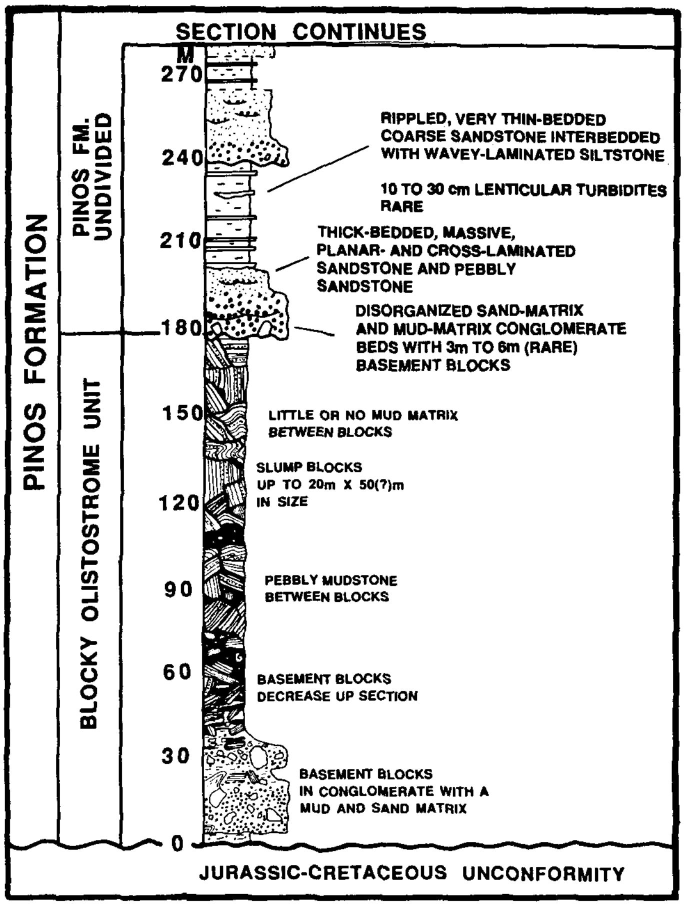

Figure 8. Measured section of basal Pinos Formation exposed between the Coloradito and Choyal faults (column "D" in Fig. 4) showing details of the blocky olistostrome unit (slope-apron deposits) and overlying undivided Pinos Formation (channel-interchannel deposits).

1 m to greater than 100 m. In addition to stacked slump blocks, very irregular patches of sand and blocks of semicoherent to coherent sandstone strata as much as tens of meters broad occur encased within featureless mudstone in these units. These chaotic deposits record episodic, generally large-scale, intrabasinal slope failures that carried slump blocks *en masse* out into the basin. The large Jurassic blocks within the basal part of the blocky olistostrome unit suggest that the flow originated near, or passed by, the foot of a fault scarp, where it could sweep the talus farther into the basin.

We interpret the above deposits as slope-apron deposits for the following reasons. (1) The slump blocks are chiefly thick mudstone, with rare thin-bedded turbidites, suggestive of a basin-plain or slope environment, but their presence within olistostromes suggests the slope-origin option. (2) The generally very great thicknesses of these deposits suggest that they came to rest at a local break in slope (Nelson, 1983) or against a backstop, such as a fault scarp. In the case of the blocky olistostrome unit, which bears large Jurassic blocks derived from scarps of the basin floor, there is a probable genetic link between the deposit and the activation of a second fault system (Coloradito fault; Fig. 3), located 3 to 4 km northwest of the Choyal fault, as discussed in the next section.

PLATE TECTONICS AND BASIN STRUCTURE

We envision that the phase two and phase three deposits filled a half-graben structure bounded on the northwest by the Choyal fault in early Cenomanian time, and by the Coloradito fault thereafter. Modern structural canyons of the Aleutian convergent margin (Fig. 9; Geist and others, 1988) may provide a physical model for the half graben on Cedros Island. The Aleutian canyons formed in response to oblique convergence that rotated and extended crustal blocks in the arc and fore-arc region (Geist and others, 1988). In another modern example of fore-arc extension, oblique convergence along the Kuril margin has opened a large graben structure that forms a submarine canyon linking the fore-arc and trench regions (Kimura, 1986). In the Kuril example, oblique convergence between the Pacific and Asian plates has de-

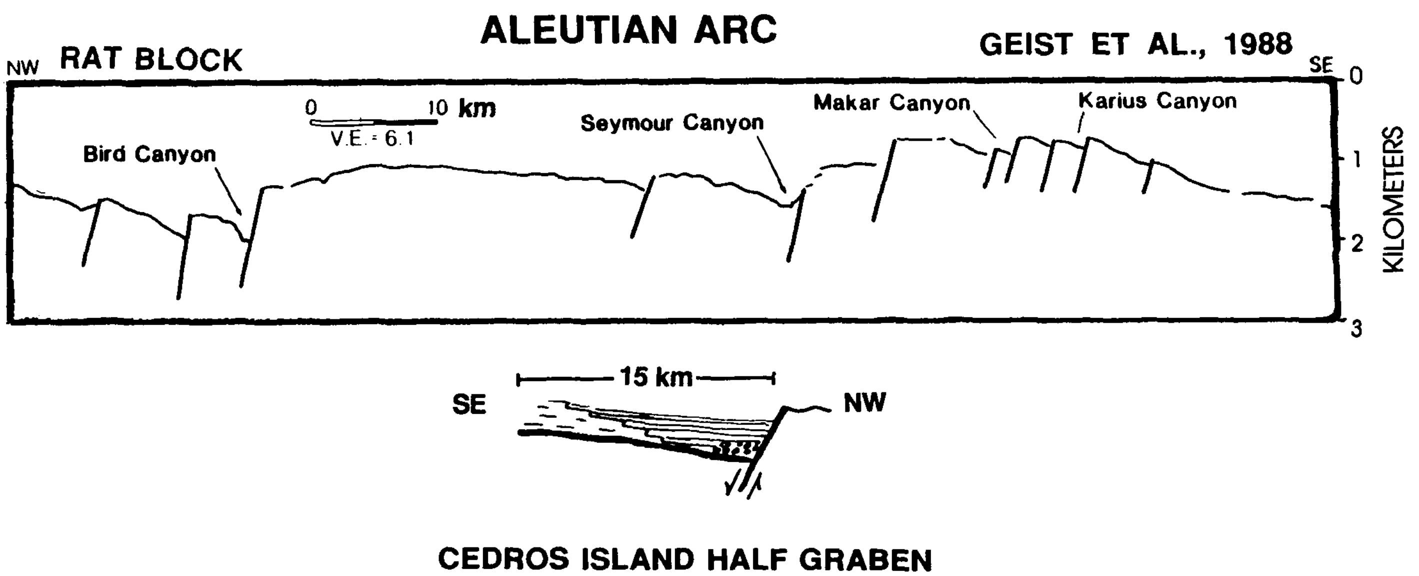

Figure 9. Half-graben structures in the Aleutian convergent margin form submarine canyons of the same scale (compare Seymour Canyon) as the inferred Cretaceous example on Cedros Island.

tached a fore-arc sliver from the Asian plate and has driven it southward, extending the crust at the trailing edge of the sliver (Kimura, 1986). Plate reconstructions suggest that right-lateral oblique convergence prevailed along the western North American margin in mid-Cretaceous time (Engebretsen and others, 1985; Hagstrum and Sedlock, 1990), and this may have driven the extension recorded in the Valle Group of Cedros Island.

Implications for Models of Blueschist Uplift

Recent models of blueschist uplift suggest that metamorphic rocks are uplifted in the hanging walls of normal faults soon after metamorphism. Underplating of the continental margin provides upward mobility, and coeval unroofing brings the blueschists to the Earth's surface (Platt, 1986; Harms and others, 1992). Uplift of late Mesozoic blueschist rocks in the California Coast Ranges is weakly constrained to have begun no earlier than Late Cretaceous time (Jayko and others, 1987; Harms and others, 1992), and the first high-relief exposures of blueschist basement along the convergent margin are inferrable from the abundance of blueschist clasts within early and middle Miocene sedimentary deposits of the Southern California borderland (Page, 1981). A similar uplift history is evident on Cedros Island. The onset of Cretaceous extension on Cedros Island is marked by the breccia unit of the Pinos Formation (Fig. 2), which lies along the Choyal fault at the same stratigraphic level as early Cenomanian beds of the sandstone unit in Gran Cañon (Fig. 2; Smith and others, in press). Normal faulting along the Coloradito fault is linked to the age of the blocky olistostrome unit of the Pinos Formation, which formed by catastrophic slope failure between middle Cenomanian time (age of the youngest known dated slump block) and early Coniacian time (oldest age limit on overlying deposit; Smith and others, in press). Thus the age of initial extension is constrained to middle Cretaceous time. Coarse-grained blueschist sediment first appeared on Cedros Island in late Miocene or early Pliocene time, further suggesting a comparable uplift history along the plate margin between Cedros Island and the California Coast Ranges.

The onset of faulting on Cedros Island (early Cenomanian) may be tied to an initial phase of crustal attenuation associated with uplift of blueschist-grade metamorphic rocks now exposed in structural windows cut through the Valle Group (Sedlock, 1988a, 1988b, 1988c; Baldwin and Harrison, 1989, 1992). Blueschist-grade metamorphic rocks exposed on Cedros Island (JKm of Fig. 1) constitute the exhumed lower plate of the Cretaceous convergent margin (Sedlock, 1988a, 1988b, 1988c). These rocks reached maximum burial and peak blueschist conditions sometime between 115 and 94 Ma (Baldwin and Harrison, 1989). Since that time, 5 to 20 km of crustal attenuation has brought the rocks to the surface (Sedlock, 1988a). This crustal thinning produced ubiquitous normal faults in rocks of the upper plate, especially in the Valle Group sediments. The near coincidence of peak metamorphism in the lower plate of the convergent margin and the onset of extensional features in the upper plate (that is, syndepositional faulting in the fore-arc basement reported here at ca. 95 Ma) support blueschist unroofing models calling for uplift soon after peak metamorphism (for examples, Platt, 1986; Jayko and others, 1987).

Local Controls on Fault Location and Orientation

Insofar as brittle faulting of the upper crust is dynamically related to more ductile deformation at depth during blueschist uplift, kinematic strain indicators produced in both regimes should have similar orientations. A comparison of strain orientation in upper- and lower-plate rocks on Cedros Island would test the hypothesis that they were deformed by the same stress field. We do not recommend such a comparison on Cedros Island because fault position and orientation were likely controlled more by local crustal inhomogeneity than by stress orientation.

A major control on Cretaceous fault orientation and location within the basin was structural heterogeneity in Middle Jurassic rocks forming the basin floor. The Choyal fault, which was active in Cretaceous time, may have first accommodated Middle Jurassic island-arc rifting. Middle Jurassic basement rocks are divided into island-arc magmatic rocks, exposed north of the Choyal fault (Ja of Fig. 1) and ophiolite, exposed south of the mouth of Gran Cañon (Jo of Fig. 1; Kimbrough, 1982, 1985). A Middle Jurassic marine volcaniclastic apron (part of Js of Fig. 1) overlaps both the arc and ophiolite rocks, demonstrating that the two basement terranes are cogenetic, rather than structurally juxtaposed (Kimbrough, 1984; Busby-Spera, 1988). The contact between the arc and ophiolite rocks is not exposed, but the Choyal fault separates exposures of the two basement types, suggesting that the fault was initially an active part of the rift margin between the arc and back-arc settings (Figs. 10, 6A). Even if the Choyal fault was not active in Jurassic time, it exploited the approximate contact between the ophiolite and arc rocks. The contact between thickened, more buoyant arc lithosphere and denser ophiolite lithosphere is likely weaker than more homogeneous parts of the basin floor, and its orientation likely controlled the orientation of the Choyal fault.

The Choyal-Coloradito Fault System: An Upper Cretaceous Transfer Zone?

Overlap between the two basin-bounding faults (Choyal fault and Coloradito fault, Fig. 3) may have developed a strain-transfer zone (Morely and others, 1990) that generated catastrophic slope failure by tilting of the basin floor. Well-studied modern extensional basins such as the East African rift (Ebinger, 1989a, 1989b) and the North Sea (Lliffe and others, 1991; Morley and others, 1990) display a very complex network of overlapping and intersecting fault splays along graben margins, rather than single continuous throughgoing faults. Morley and others (1990) suggested several ways for strain to be transferred from one fault splay to another along graben margins. The initiation of the Coloradito fault produced an overlapping, synthetic transfer zone (Fig. 11, *sensu* Morley and others, 1990) that substantially tilted the intervening basin floor to the southwest, causing the Cretaceous sedimentary section to fail catastrophically. This resulted in deposition of the blocky olistostrome unit of the Pinos Formation (Figs. 3, 11).

The geometry depicted in Figure 11 requires that (1) the Coloradito fault dies to the northeast, (2) the Choyal fault dies toward the southwest, and (3) the intervening structural block is tilted to the southwest at a greater angle than is the block to the southeast of the Choyal fault:

(1) The Coloradito fault trace becomes less distinct in the field with distance to the northwest (Busby-Spera, 1988; see Fig. 3).

(2) Two points of evidence suggest that offset on the Choyal fault dies to the southwest. First, the Choyal fault has between ~500 m and 800 m of dip separation on the Jurassic-Cretaceous unconformity at the mouth of Arroyo Choyal (Fig. 3). The fault is easily mapped between the mouth of Arroyo Choyal and a point about 4 km south

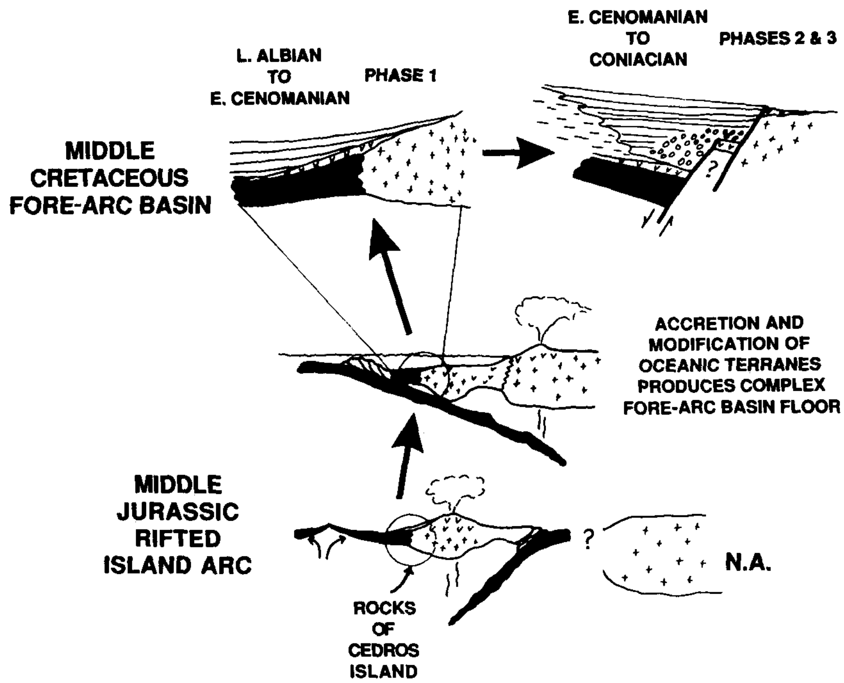

Figure 10. Cartoon showing the simplified tectonic history of Cedros Island. The structural join (Choyal fault; Fig. 1) between Jurassic island arc (crosses and v's) and Jurassic ophiolite (black) was exploited as a zone of weakness during the "middle" Cretaceous extension that downdropped the northern margin of the fore-arc basin in phase two of the basin evolution.

of Arroyo Coloradito (Fig. 3); farther south, the trace is lost (buried?) within strata of the undivided Pinos Formation (Fig. 3). Second, seismically imaged graben-margin deposits are commonly depicted with an axial syncline structure of comparable scale to the Pinos syncline, first mapped by Kilmer (1984; see Fig. 3; compare with Viking graben margin in Fig. 3 of Khalid and Damuth, 1987). The Pinos syncline is well expressed southeast of good traces of the Choyal fault, but it dies toward the southwest approximately where the Choyal fault becomes hard to track (Fig. 3).

(3) The Middle Jurassic Gran Cañon Formation, which is part of the Cretaceous basin-floor assemblage, dips southwest on average 20° more between the Coloradito and Choyal faults (Fig. 3) than it does on the southeast side of the Choyal fault, near the mouth of Arroyo Choyal (Fig. 3). Unlike the Jurassic strata, Cretaceous strata from those two localities have approximately equal dip magnitudes (Fig. 3), suggesting that differential tilting of the Jurassic strata at least predates deposition of Cretaceous strata between the faults (approximately late Cenomanian; Fig. 5), and may predate Cretaceous strata at the mouth of Arroyo Choyal (early Cenomanian).

Morley and others (1990) emphasized that transfer zones with overlapping faults can be excellent hydrocarbon traps. Although there are no hydrocarbon plays known in the Valle Group, the thick interstratification of slumped shale horizons and turbidite sequences that characterizes the transfer zone fill exposed on Cedros Island (Fig. 3) would likely make an excellent hydrocarbon source and reservoir system, given proper maturation.

CONCLUSIONS

The three-phase sedimentological and structural evolution of the Cretaceous basin on Cedros Island (Fig. 6) was dominated by tectonic activity, likely stemming from its position outboard from the arc, close to the edge of the convergent margin (Morris and others, 1987). Although half grabens of the Aleutian convergent margin (Fig. 9) are good physical analogues for the structural basin inferred here, the sedimentology of their fill is very poorly known. The facies distribution in the half-graben (phase two; Fig. 6B) deposits of Cedros Island is partly analogous to that in Jurassic deposits within the southern

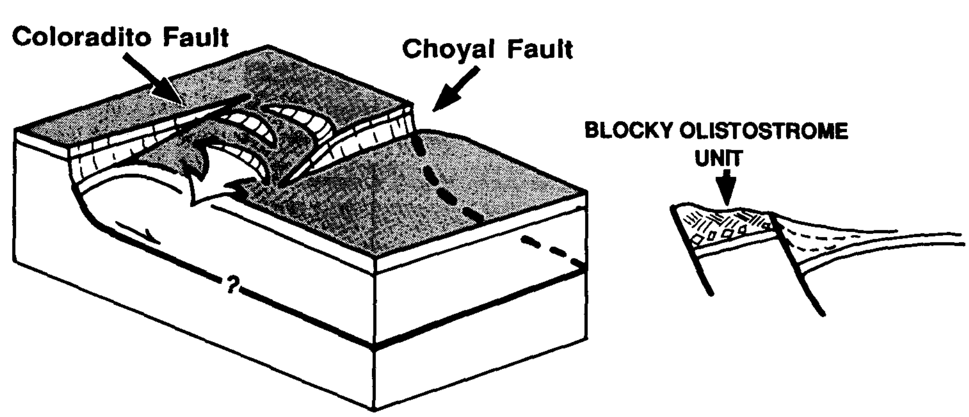

Figure 11. Schematic block model (after Morley and others, 1990) of overlapping synthetic normal faults. The intervening block is a structural accommodation zone ("transfer zone" of Morley and others, 1990). Faults and deposits are labeled.

Viking Graben (Turner and others, 1987). Interstratified channel-interchannel and slope-apron deposits (phase three; Fig. 6C) are in some respects similar to part of the modern Ebro turbidite complex which lies in a tectonically active basin in the Mediterranean Sea (Alonso and others, 1991).

In phase one of the basin history, a channeled slope environment fed sand-rich turbidity currents downslope to the south-southeast to a sand-rich submarine fan that aggraded on a basin-plain environment (Fig. 6A). In detail, the proximal edge of the system was first a thin veneer of basin-plain mudstone that lapped onto a basement paleohigh, which sloped down to the southeast (Fig. 6A). Sediment-gravity flows sourced in the north-northwest built channel-topped lobes that prograded downslope onto the basin-plain deposits (for example, as in Fig. 7B). Numerous channels then fed sand directly onto a basin-plain environment that had previously been sand starved. The turbidity currents aggraded into a thick, wedge-shaped deposit that bears evidence of construction by both channel and lobe processes (Fig. 6A). This sudden pulse of sediment may have been driven by a sea-level cycle of appropriate age (early Cenomanian, 3rd-order cycle 2.3 of Haq and others, 1987). Between phase one and phase two times, substantial tilting of the basin floor resulted in a major change in paleocurrent direction (Figs. 3, 4).

In phase two time, a voluminous influx of gravel and sand, derived from an arc provenance to the east (Fig. 1A), filled a syndepositionally active half-graben structure bounded on the northwest by scarps of the Choyal fault (Fig. 6B). Paleocurrents in strata adjacent to the Choyal fault show that the axis of the half graben directed sediment-gravity flows longitudinally, like in a submarine canyon. Large-volume sediment-gravity flows were able to spread laterally up the gently northwestwardly inclined half-graben floor, leaving deposits in the axis, proximal-shoulder, and distal-shoulder environments on the hanging wall (Fig. 6B).

The phase two half-graben fill may be an excellent outcrop analogue for the hydrocarbon-rich Brae Formation of the Viking Graben, which is known only from subsurface studies. The cross-sectional distribution of phase two lithofacies (Fig. 5) is similar to that shown on an east-west profile of the Brae Formation, transverse to the Viking Graben (Turner and others, 1987). Turner and others (1987) recognized three facies associations that are largely analogous to the tripartite division described here in phase two deposits (Fig. 5). In detail, conglomeratic facies in the Brae are restricted mainly to a zone within 3 to 4 km from the Viking Graben faults; the conglomerate facies interfinger with sandstone facies that spread laterally across the graben floor, prograding away from the fault scarp as sedimentation rates outpaced tectonic subsidence rates of the graben floor. This situation is directly comparable with the phase two system on Cedros Island (Figs. 5, 6B). The major geometric difference between the two basins is that the Cedros Island example was a longitudinally drained half graben, whereas the sediment-gravity flows in the Brae Formation are inferred to have flowed chiefly transverse to the graben margin. The phase two deposits are much thinner than the Brae Formation because the Viking Graben margin dwarfs the Choyal fault in both physical and temporal scales.

In phase three time, the axis of the half graben gradually filled, and channels were no longer confined to the axial depression. Channels migrated southeastward, leaving broad deposits of aggraded channel and interchannel deposits (Fig. 6C). Evidence for continued seismicity in the basin during phase three is (1) the presence of Jurassic blocks in conglomerate sporadically throughout the section, and within the blocky olistostrome unit of the Pinos Formation (Fig. 8), which likely marks the onset of activity on the Coloradito fault, and (2) abundant sediment-failure features, including thick, slope-apron deposits.

Phase three channel-interchannel deposits are difficult to interpret because they bear no typical fan organization, and their lateral continuity is disrupted by faults. The bipartite association of thick sections of thin-bedded, rippled sandstone interstratified with conglomerate and thick-bedded sandstone is like the "middle-fan" facies association of Mutti and Ricci Lucchi (1972); however, we hesitate to use idealized submarine-fan terms for these deposits because we cannot relate them to other coeval submarine-fan environments for context.

Phase three deposits may be comparable to the interstratified "channel-levee complexes" and "apron deposits," seismically imaged in the Ebro turbidite complex (Nelson and Maldonado, 1988; Alonso, and others, 1991). The comparison holds in the existence of thickly interstratified interchannel deposits (whether or not they have levee morphology) and slope-apron deposits of similar scale. Some of the "apron" deposits in the Ebro section (Nelson and Maldonado, 1988) show evidence of having deeply scoured into the substrate. Outcrops of slope-apron deposits on Cedros Island show that such erosion may proceed rapidly via mud sills that inject and detach large rafts of strata (tens of meters), rather than via grain-by-grain disaggregation of the substrate. We emphasize that although certain physical details of the two systems are analogous, the scale of the Ebro system is far greater than the scale of observation on Cedros Island. Each "channel-levee complex" of the Ebro system is about 15 km wide (Nelson and Maldonado, 1988), as wide as the entire exposure of the Valle Group on Cedros Island (Fig. 1).

Extension of the fore-arc basement is recorded in the fault-generated, early Cenomanian phase two deposits. Thus Platt's (1989) model of rapid blueschist uplift is supported in western central Baja California by the close timing between brittle extension in the upper plate and peak metamorphism in the lower plate of the convergent margin.

ACKNOWLEDGMENTS

We gratefully thank Keith Berry (Consulting Micropaleontologist), LouElla Saul and John Alderson (Los Angeles Natural History Museum), and Mark Filewicz (Unocal) for their paleontological assistance. We thank R. L. Sedlock for discussions of Cedros Island blueschists. Sedlock and David Kimbrough generously provided aerial photographs for field mapping. Careful manuscript reviews by Kimbrough and D. W. Andersen greatly improved the scope and content of the paper. Our Mexican liaisons, Jorge Ledesma and Francisco Suarez, are acknowledged for fostering our work in their country. Field assistants included Scott Renger, Karen McCormack, Karen Maley, and Brian Steele. We especially thank Manuel Aguilar and Francisco Villa (Domicilio Conocido, Isla Cedros) for their hospitality and logistical support in the field. U.N.A.M. (Mexico City) provided collection permits for rocks and fossils. The following institutions generously provided financial support for this work: National Science Foundation (EAR83-13226 to Busby-Spera and Boles; EAR86-18771 to Busby-Spera; EAR9116438 to Smith and Busby-Spera); Geological Society of America; British Petroleum (gift to Busby-Spera); Unocal (Ventura); and grateful acknowledgment is given to the donors of the Petroleum Research Fund of the American Chemical Society.

REFERENCES CITED

Alonso, B., Canals, M., Got, H., and Maldonado, A., 1991, Sea valleys and related depositional systems in the Gulf of Lion and Ebro continental margins: American Association of Petroleum Geologists Bulletin, v. 75, p. 1195–1214.

Baldwin, S. L., and Harrison, T. M., 1989, Geochronology of blueschists from west-central Baja California and the timing of uplift in subduction zones: Journal of Geology, v. 97, p. 149–163.

Baldwin, S. L., and Harrison, T. M., 1992, The P-T-t history of blocks in serpentinite-matrix mélange, west-central Baja California: Geological Society of America Bulletin, v. 104, p. 18–31.

Barnes, D. A., 1984, Volcanic arc derived, Mesozoic sedimentary rocks, Vizcaino Peninsula, Baja California Sur, Mexico, *in* Frizzell, V. A., Jr., ed., Geology of the Baja California Peninsula: Society of Economic Paleontologists and Mineralogists, Pacific Section, v. 39, p. 119–130.

Boles, J. R., and Landis, C. A., 1984, Jurassic sedimentary mélange and associated facies, Baja California, Mexico: Geological Society of America Bulletin, v. 95, p. 513–521.

Busby-Spera, C. J., 1985, A sand-rich submarine fan in the lower Mesozoic Mineral King caldera complex, Sierra Nevada, California: Journal of Sedimentary Petrology, v. 55., p. 376–391.

Busby-Spera, C. J., 1988, Evolution of a Middle Jurassic back-arc basin, Cedros Island, Baja California: Evidence from a marine volcaniclastic apron: Geological Society of America Bulletin, v. 100, p. 218–233.

Busby-Spera, C. J., and Boles, J. R., 1986, Sedimentation and subsidence styles in a Cretaceous fore arc basin, southern Vizcaino Peninsula, Baja California, (Mexico), *in* Abbott, P. L., ed., Cretaceous stratigraphy of western North America: Society of Economic Paleontologists and Mineralogists, Pacific Section, v. 46, p. 79–90.

Ebinger, C. J., 1989a, Geometric and kinematic development of border faults and accommodation zones, Kivu Rusizi rift, Africa: Tectonics, v. 8, p. 117–133.

Ebinger, C. J., 1989b, Tectonic development of the western branch of the east African rift system: Geological Society of America Bulletin, v. 101, p. 885–903.

Engebretsen, D. C., Cox, A., and Gordon, R. G., 1985, Relative motions between oceanic and continental plates in the Pacific basin: Geological Society of America Special Paper 206, 59 p.

Gastil, R. G., Morgan, G. J., and Krummenacher, D., 1978, Mesozoic history of peninsular California and related areas east of the Gulf of California, *in* Howell, D. G., and McDougall, K. A., eds., Mesozoic paleogeography of the western United States: Society of Economic Paleotologists and Mineralogists, Pacific Section, Pacific Coast Paleogeography symposium 2, p. 107–115.

Geist, E. L., Childs, J. R., and Scholl, D. W., 1988, The origin of summit basins of the Aleutian ridge: Implication for block rotation of an arc massif: Tectonics, v. 7, p. 327–341.

Graham, S. A., and Bachman, S. B., 1983, Structural controls on submarine-fan geometry and internal architecture: Upper La Jolla fan system, offshore Southern California: American Association of Petroleum Geologists Bulletin, v. 67, p. 83–96.

Hagstrum, J. T., and Sedlock, R. L., 1990, Remagnetization and northward translation of Mesozoic red chert from Cedros Island and the San Benito Islands, Baja California, Mexico: Geological Society of America Bulletin, v. 102, p. 983–991.

Haq, B. U., Hardenbol, J., and Vail, P. R., 1987, Chronology of fluctuating sea levels since the Triassic: American Association for the Advancement of Science, v. 235, p. 1156–1167.

Harms, T. A., Jayko, A. S., and Blake, M. C., 1992, Kinematic evidence for extensional unroofing of the Franciscan complex along the Coast Range fault, northern Diablo Range, California: Tectonics, v. 11, p. 228–241.

Harris, J. P., and Fowler, R. M., 1987, Enhanced prospectivity of the mid-Late Jurassic sediments of the South Viking Graben, northern North Sea, *in* Brooks, J., and Glennie, K., eds., Petroleum geology of northwest Europe: Boston, Massachusetts, Graham and Trotman, p. 879–898.

Jayko, A. S., Blake, M. C., and Harms, T., 1987, Attenuation of the Coast Range ophiolite by extensional faulting, and nature of the Coast Range "thrust," California: Tectonics, v. 6, p. 475–488.

Jones, D. L., Blake, M. C., Jr., and Rangin, C., 1976, The four Jurassic belts of northern California and their significance to the geology of the southern California borderland, *in* Howell, D. G., ed., Aspects of the geologic history of the California continental borderland: American Association of Petroleum Geologists Miscellaneous Publication 24, p. 343–362.

Khalid, A., and Damuth, J. E., 1987, Slide block (?) of Jurassic sandstone and submarine channels in the basal Upper Cretaceous of the Viking Graben: Norwegian North Sea: Marine and Petroleum Geology, v. 4, p. 35–48.

Kilmer, F. H., 1984, Geology of Cedros Island, Baja California, Mexico [Ph.D. dissert.]: Arcata, California, Humboldt State University, 69 p.

Kimbrough, D. L., 1982, Structure, petrology, and geochronology of Mesozoic paleooceanic basement terranes on Cedros Island and the Vizcaino Peninsula [Ph.D. dissert.]: Santa Barbara, California, University of California, 395 p.

Kimbrough, D. L., 1984, Paleogeographic significance of the Middle Jurassic Gran Canon Formation, Cedros Island, Baja California Sur, *in* Frizzell, V. A., Jr., ed., Geology of the Baja California Peninsula: Society of Economic Paleontologists and Mineralogists, Pacific Section, v. 39, p. 107–117.

Kimbrough, D. L., 1985, Tectonostratigraphic terranes of the Vizcaino Peninsula and Cedros and San Benito Islands, Baja California, Mexico, *in* Howell, D. G., ed., Tectonostratigraphic terranes of the circum-Pacific region: Houston, Texas, Circum-Pacific Council for Energy and Mineral Resources, p. 285–298.

Kimura, G., 1986, Oblique subduction and collision: Fore-arc tectonics of the Kuril arc: Geology, v. 14, p. 104–107.

Leeder, M. R., and Gawthorpe, R. L., 1987, Sedimentary models for extensional tilt-block/half-graben basins, *in* Coward, M. P., Dewey, J. F., and Hancock, P. C., eds., Continental extension tectonics: Geological Society [London] Special Publication, no. 28, p. 139–152.

Link, M. H., and Nilsen, T. H., 1980, The Rocks Sandstone, an Eocene deep-sea fan deposit, northern Santa Lucia Range, California: Journal of Sedimentary Petrology, v. 50, p. 583–602.

Lliffe, J. E., Lerche, I., and Cao, S., 1991, Basin analysis predictions of known hydrocarbon occurrences: The North Sea Viking Graben as a test case: Earth Sciences Reviews, v. 30, p. 51–80.

Lowe, D. R., 1982, Sediment gravity flows II: Deposition models with special reference to the deposits of high-density turbidity currents: Journal of Sedimentary Petrology, v. 52, p. 279–297.

McClean, H., and Howell, D. G., 1985, Blanca turbidite system, California, *in* Bouma, A. H., Normark, W. R., and Barnes, N. E., eds., Submarine fans and related turbidite systems: New York, Springer-Verlag, p. 167–172.

Moore, T. E., 1985, Stratigraphy and tectonic significance of the Mesozoic tectonostratigraphic terranes of the Vizcaino Peninsula, Baja California Sur, Mexico, *in* Howell, D. G., ed., Tectonostratigraphic terranes of the circum-Pacific region: Houston, Texas, Circum-Pacific Council for Energy and Mineral Recources, p. 315–329.

Morley, C. K., Nelson, R. A., Patton, T. L., and Munn, S. G., 1990, Transfer zones in the east African rift system and their relevance to hydrocarbon exploration in rifts: American Association of Petroleum Geologists Bulletin, v. 74, p. 1234–1253.

Morris, W. R., and Busby-Spera, C. J., 1990, A submarine fan valley-levee complex in the Upper Cretaceous Rosario Formation, Baja California: Implications for turbidite facies models: Geological Society of America Bulletin, v. 102, p. 900–914.

Morris, W. R., Smith, D. P., and Busby-Spera, C. J., 1989, Deep marine conglomerate facies and processes in Cretaceous fore-arc basins of Baja California, Mexico, *in* Colburn, I. P., Abbott, P. L., and Minch, J., eds., Conglomerates in basin analysis: A Symposium Dedicated to A. O. Woodford: Society of Economic Paleontologists and Mineralogists, Pacific Section, v. 62, p. 123–142.

Mutti, E., 1979, Turbidites et cones sous-marins profonds, *in* Homewood, P., ed., Sédimentation Détritique (Fluviatile, Littorale et Marine): Institut de Géologie, Université de Friborg, Suisse, p. 353–419.

Mutti, E., and Normark, W., 1987, Comparing examples of modern and ancient turbidite systems: Problems and concepts, *in* Leggett, J. K., and Zuffa, G. G., eds., Marine clastic sedimentology: Boston, Massachusetts, Graham and Trotman, p. 1–38.

Mutti, E., and Ricci Lucchi, F., 1972, Turbidites of the northern Apennines: Introduction to facies analysis (English translation by T. H. Nelsen, 1978): International Geology Review, v. 20, p. 125–166.

Nelson, C. H., 1983, Modern submarine fans and debris aprons: An update of the first half century, *in* Boardman, S. J., ed., Revolution in the Earth sciences: Advances in the past half-century: Dubuque, Iowa, Kendall/Hunt, p. 148–166.

Nelson, C. H., and Maldonado, A., 1988, Factors controlling depositional patterns of Ebro turbidite systems, Mediterranean Sea: American Association of Petroleum Geologists Bulletin, v. 72, p. 698–716.

Normark, W. R., Piper, D.J.W., and Hess, G. R., 1979, Distributary channels, sand lobes, and mesotopography of Navy submarine fan, California borderland, with applications to ancient fan sediments: Sedimentology, v. 26, p. 749–774.

Page, B. M., 1981, The southern Coast Ranges, *in* Ernst, W. G., ed., The geotectonic development of California: Englewood Cliffs, New Jersey, Prentice-Hall, p. 329–417.

Patterson, D. L., 1984, Los Chapunes and Valle Sandstones: Cretaceous petrofacies of the Vizcaino basin, Baja California, Mexico, *in* Frizzell, V. A., Jr., ed., Geology of the Baja California Peninsula: Society of Economic Paleontologists and Mineralogists, Pacific Section, v. 39, p. 161–182.

Pickering, K., Stow, D., Watson, M., and Hiscott, R., 1986, Deep water facies, processes and models: A review and classification scheme for modern and ancient sediments: Earth Science Reviews, v. 23, p. 75–174.

Platt, J. P., 1986, Dynamics of orogenic wedges and the uplift of high-pressure metamorphic rocks: Geological Society of America Bulletin, v. 97, p. 1037–1053.

Sedlock, R. L., 1988a, Lithology, petrology, structure, and tectonics of blueschists and associated rocks in west-central Baja California, Mexico [Ph.D. dissert.]: Stanford, California, Stanford University, 223 p.

Sedlock, R. L., 1988b, Metamorphic petrology of a high-pressure, low-temperature subduction complex in west-central Baja California, Mexico: Journal of Metamorphic Petrology, v. 6, p. 205–233.

Sedlock, R. L., 1988c, Tectonic setting of blueschist and island-arc terranes of west-central Baja California, Mexico: Geology, v. 16, p. 623–626.

Shanmugam, G., and Moiola, R. J., 1988, Submarine fans: Characteristics, models, classification, and reservoir potential: Earth-Science Reviews, v. 24, p. 383–428.

Smith, D. P., 1991, Lithostratigraphy, sedimentology, and paleomagnetism of the Cretaceous Valle Group, Cedros Island, Baja California, México [Ph.D. dissert.]: Santa Barbara, California, University of California, 192 p.

Smith, D. P., Sedlock, R. L., Kimbrough, D. L., and Busby-Spera, C. J., 1991, Mesozoic geology of Cedros Island, *in* Walawender, M., and Hannon, B., eds., Geological excursions in Southern California and Mexico: San Diego, California, Geological Society of America 1991 Annual Meeting Guidebook, p. 332–348.

Smith, D. P., Busby-Spera, C. J., and Berry, K. D., 1992, Lithostratigraphy of Cretaceous strata, Cedros Island, Baja California, Mexico: Journal of Cretaceous Research (in press).

Spencer, J. E., and Normark, W. R., 1989, Neogene plate-tectonic evolution of the Baja California Sur continental margin and southern Gulf of California, Mexico: The Geology of North America, Volume N, The eastern Pacific Ocean and Hawaii: Boulder, Colorado, Geological Society of America, p. 489–497.

Stow, D. A., Bishop, C. D., and Mill, S. J., 1982, Sedimentology of the Brae oilfields, North Sea: Fan models and controls: Journal of Petroleum Geology, v. 5, p. 129–148.

Turner, C. C., Cohen, J. M., Connell, E. R., and Cooper, D. M., 1987, A depositional model for the South Brae oilfield, *in* Brooks, J., and Glennie, K., eds., Petroleum geology of northwest Europe: Boston, Massachusetts, Graham and Trotman, p. 853–864.

Manuscript Received by the Society October 25, 1991
Revised Manuscript Received September 30, 1992
Manuscript Accepted October 12, 1992

Printed in U.S.A.